INTERNATIONAL JOURNAL OF SUSTAINABLE CONSTRUCTION ENGINEERING AND TECHNOLOGY
VOL. 14 NO. 4 (2023) 332-353

IJSCET

http://publisher.uthm.edu.my/ojs/index.php/ijscet

ISSN : 2180-3242 e-ISSN : 2600-7959

International Journal of Sustainable Construction Engineering and Technology

Effects of Industrial and Agricultural Recycled Waste Enhanced with Lime Utilisation in Stabilising Kaolinitic Soil

Muhammad Syamsul Imran Zaini[1], Muzamir Hasan[1*]

[1]Faculty of Civil Engineering Technology, Universiti Malaysia Pahang,
Lebuh Persiaran Tun Khalil Yaakob, Kuantan, 26300, MALAYSIA

*Corresponding Author

DOI: https://doi.org/10.30880/ijscet.2023.14.04.025
Received 02 April 2023; Accepted 13 December 2023; Available online 28 December 2023

Abstract: Soft kaolin clay is a problematic soils encountered in various construction projects that lead to the implementation of soil stabilisation. On the other side, the massive production of industrial and agricultural waste currently presents a critical problem for the environment. However, the utilisation of industrial and agricultural wastes in altering the characteristics of kaolinitic soil can be considered as an ideal solution to enhance the characterisation of problematic soils in the field of construction. Therefore, this study examines the alterations of the engineering properties of soft kaolin clay by utilising silica fume as the industrial by-product and eggshell ash as the agricultural by-product enhanced with lime use. To assess the impact of silica fume, eggshell ash, and lime on the various characteristics of kaolinitic soil, a series of laboratory experiments containing Atterberg limits, specific gravity, compaction test, unconfined compression test, X-ray fluorescence, X-ray diffraction, sieve analysis, and field emission scanning electron microscope is carried out. In this study, 2%, 4% and 6% of silica fume, 3%, 6% and 9% of eggshell ash and lime and the optimal combination of SF, ESA with 3%, 6% and 9% of lime are used and were cured for 1, 7, 14 and 30 days. The results present that the optimal utilization of silica fume, eggshell ash, and lime can alter the engineering characteristics of the soft kaolin clay by reducing the specific gravity, consistency limits, linear shrinkage, and maximum dry density, while increasing the value of shrinkage limit, and optimum moisture content. In terms of strength improvement, the highest unconfined compression strength was recorded when soft kaolin clay was treated with 6% silica fume, 6% eggshell ash and 9% of lime for four (4) different days of curing with a strength improvement of 81.03%, 82.46%, 88.49% and 88.74%. Therefore, this study concludes that optimal use of silica fume, eggshell ash, and lime can persistently alter the characteristics of kaolinitic soil and open the way to economical and sustainable materials in improving the problem soil.

Keywords: Eggshell ash, lime, silica fume, soft kaolin clay, soil improvement

1. Introduction

Kaolinitic soil is among the complex soils faced in construction projects (Ishak & Zaini, 2018) and recognized for its problematic characteristics due to the volumetric alterations corresponding to the modifications in the dampness regime (Goh et al., 2020). Some of the main engineering characteristics and resistance problems associated with these soil forms include severe settlement, low welding resistance, insufficient plasticity, greater compressibility, dispersion, expansion, erosion, and resistance to climate variables (Hasan et al., 2021a). Furthermore, the consequent calamities and estimated expenses of recovery and reconstruction of structures based on the problematic soils are a national concern (Zolkepli et al., 2019). Kaolin among the most common types of clay minerals (Zolkepli et al., 2018). Kaolin are the most sensitively distributed high-resistance clays between each other (Zaini et al., 2023). Hence, unstable soils,

*Corresponding author: muzamir@ump.edu.my

such as soft clay soils, were altered to change technical properties and increase soil cutting strength (Araujo et al., 2023). For this reason, previous researchers suggested several methods, such as soil stabilization (Ishak et al., 2021), soil improvement, (Hasan et al., 2021b) and, etc. in altering the characteristics of kaolinitic soils.

Soil improvement is executed to allow improving the existing material characteristics to satisfy the construction designation (Ali et al., 2022). Among the latest approach to soil improvement is to substitute disconcerted soil with material such as concrete, geotextiles, and geocross sections (Hilal & Hadzima-Nyarko, 2021). Recent investigations have highlighted the use of waste from industrial in various development projects as a cost-effective construction supplies option (Zaini & Hasan, 2023). Many researches focus on the utilisation of industrial waste, such as fibre waste, sludge, fly dust, rubber chips, etc. as a substitutes for soil improvement (Zolkepli et al., 2021). Furthermore, previous researchers have also focused on the utilisation of pozzolan in the manufacture of composite cement. Pozzolan, for example, igneous ash (Bagriacik, 2021) and fly ash (Yue et al., 2019; Zaini et al., 2020a) are notable additional cement substitution materials owing to the rich content in silica, substantial availability, and manifest pozzolanic responsiveness. Nevertheless, agrodegradable products have currently captivate the attention of researchers owing to the enormous availability of waste in this field (Zaini et al., 2019; Zaini et al., 2020b).

Therefore, the agroresidue material utilized as soil improvement binder is eggshell waste (ESA). Egg shells commonly called calcite ($CaCO_3$) contain calcium carbonate (Mohammed et al., 2021) can be used to decrease cement in concrete manufacturing (Hamada et al., 2020). There is a minor growth in egg production around the world and it is essential to deliver an overabundance of more than 9 million tons of eggshell waste every year (Sathiparan, 2021). The total number of eggs consigned in Canada and France is by and large more than 2 billion and 1 billion individually. Prudently, 6500 tons of calcium carbonate powder are imparted from 1 billion eggs (Tiong et al., 2020). 8979 million eggs were depleted in 2011 and this figure had been enlarged to 12235 million eggs in 2017 and it is required to rise strenuously in the imminent years (Poorvekan et al., 2021). Approximately 150 thousand tons of eggshell waste is conceived in dumpsites (Zaini et al., 2022b). Therefore, it could be shown that as the common inhabitants continue to produce, eggshell waste increases substantially (Ofuyantan et al., 2020; Brescia-Norambuena et al., 2021). Hence, owing to the large generation of eggshell waste, the eggshell waste were assessed and utilised as ideal materials to alter the characteristics of kaolinitic soils blends with silica fume and lime using the soil improvement technique. Nevertheless, it is extremely difficult to discover a producer that can recycle the ESA owing to the latest material implementation utilised in the construction development projects (Hamada et al., 2020).

Consequently, the environmental benefits of egg shell ash can be linked to the elimination of the need to dispose of egg shell waste at landfills as an alternative supply of raw materials when used as a replacement for traditional fragile aggregates. Using egg shell ash as a sustainable substitute for soft clay soil to improve soils must be thoroughly understood about the characteristics of egg shell ash and its effects on the characteristics of kaolinitic soil. The utilization of silica fume and egg shell ash with lime can provide an ideal and sustainable solution in cement replacement material as it can reduce the pollution by reducing the production of waste in the landfill and reducing carbon dioxide emission to the environment. Moreover, the use of silica fume, egg shell ash, and lime can ensure that the pozzolanic reaction occurs thus forming a calcium silicate hydrate (CSH), and calcium aluminate hydrate (CAH) which can increase the durability and strength of the kaolinitic soil in soil improvement applications. Both materials from industrial waste (silica fume) and agricultural waste (egg shell ash) are used together with lime to develop a sustainable approach to improve the bearing capacity of kaolinitic soils. The silica fume and egg shell have been used with lime to reduce plasticity and increased workability and strength of the kaolinitic soils. Various engineering properties tests have been performed on treated and untreated soils to examine the effect of silica fume, egg shell ash and lime. In the study, a detailed method of the optimal utilisation of silica fume, egg shell ash, and lime to the kaolinitic soil has also been presented in the kaolinitic soil.

2. Materials and Methods

2.1 Materials

Fig. 1 illustrates the location of the kaolin, SF, ESA and lime used in the study. Kaolinite is a clay mineral that has a water-resistant polymer structure and tends to mix and wet with water and form sludge to generate uniform soft clay. The kaolin clay is purchased from Kaolin (M) Sdn. Bhd (4°9’48.6”N, 101°16’25.32”E) located in Malaysia. The S300 grade of kaolin powder was used as a material to reproduce homogeneous soft clay samples. Table 1 demonstrates the basic characteristics of the soil used in this study.

Silica fume, produced as a by-product in the production of silicon in the electrometallurgy industry, is a substance with high pozzolanic value as a result of its high content of amorphous silica. A grey-coloured-densified SF was purchased from Scancem Materials Sdn. Bhd. (3° 15' 0.396"N, 101° 42' 48.996"E), Malaysia with a specific gravity of 2.33, LL of 90.5%, PL of 80.5% and PI of 10.0%. SF is a fine material with a 56% finer sieve of 0.075mm, generated from the production of elemental silicon at 2000°C. SF, also known as mica-silica or condensed SF is a very fine pozzolan comprising mainly spherical amorphous SiO_2 (Hasan et al., 2021c). The SF used in this study was a concrete-densified SF, Scanfume, with a surface area of at least 1500m^2/kg. The reaction reactivity of pozolanic reactions is affected by the overall surface area of SF. As the total surface area is larger, the reactivity is higher (Hasan et al., 2021c).

The chicken egg shells were gathered from the restaurants in Pahang (3° 49' 0.48"N, 103° 19' 54.12"E). The ESA has a specific gravity of 2.38, LL of 27.4%, PL of 21.6%, and PI of 5.8%. It is a coarser material, only 24% finer at a 0.075 mm sieve. The massive availability of egg shell waste was the main reasons why egg shell ash was chosen as a stabiliser in this study. It is also more sustainable than other normal soil stabilisers such as cement and others (Alnunu & Nalbantoglu, 2022; Zaini et al., 2022a). Raw eggshell consists mainly of $CaCO_3$ and is converted to CaO during calcination. Additionally, there are various types of lime used in the construction industries. They are obtained by the natural limestone over a temperature of 900 °C. Lime was used as one of the soil stabilisation materials together with SF and ESA. All of the lime used in the research will be purchased from CAO Industries Sdn. Bhd. (3° 21' 4.6764"N, 101° 35' 46.0824"E) which is situated in Selangor, Malaysia. The price of lime is also affordable and reasonable.

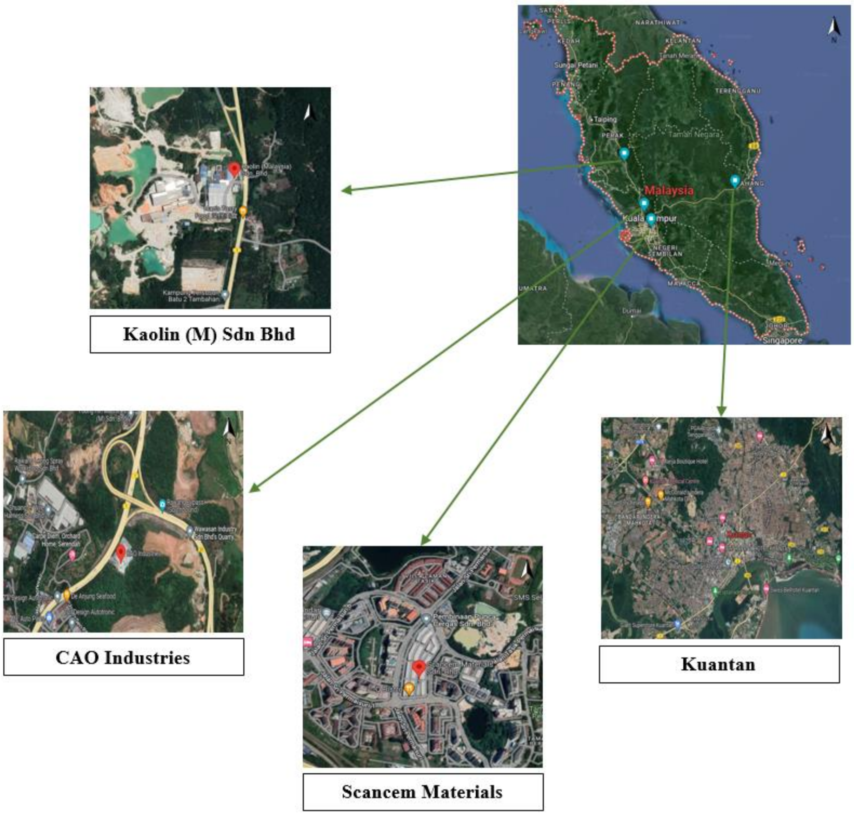

Fig. 1 - Location of kaolin clay, silica fume, eggshell ash, and lime used in this study

Table 1 - Basic Characteristics of Soft Kaolin Clay Soil

Properties	Unit	Result
Gravel	%	0
Sand	%	45
Clay and Silt	%	55
USCS		ML
AASHTO		A-7-6b
IMC	%	0.96
SG		2.62
LL	%	41
PL	%	31
PI	%	10
MDD	g/cm^3	1.58
OMC	%	18.40
Coefficient of Permeability	ms^{-1}	2.5749×10^{-8}
UCS	kPa	22.16
USS	kPa	11.08

Note: USCS, Unified Soil Classification System; AASHTO, American Association of State Highway and Transportation Officials; IMC, Initial Moisture Content; SG, Specific Gravity; LL, Liquid Limit; PL, Plastic Limit; PI, Plasticity Index; MDD, Maximum Dry Density; OMC, Optimum Moisture Content; UCS, Unconfined Compression Strength; USS, Undrained Shear Strength.

2.2 Experimental Design

2.2.1 Preparation of Sample

Laboratory tests were performed on the kaolin, SF, ESA, L, mixtures of kaolin with SF, mixtures of kaolin with SF and ESA, mixtures of kaolin with SF and lime, and mixtures of kaolin with SF, ESA and L. Soft kaolin clay was oven dried using the universal oven at 105 °C for one (1) day and after that was admixed with various percentage of SF (2%, 4% and 6%) by the overall dry weight of the soil. The kaolin-SF mix was induced with different percentages of ESA (3%, 6% and 9%) and L (3%, 6% and 9%) by the total weight of dry soil. The ESA used in this investigation was the calcined product of raw chicken egg shells that were thoroughly cleaned with tap water, followed by air drying for 7 days. The air dried egg shells were then crushed using a jaw crusher and then calcined at 800 °C for 60 minutes in the chamber furnace. The ESA was then kept in a desiccator for one (1) day for a cooling process. After that, an ESA was stored in an airtight container. The percentage of SF-ESA and SF-lime adopted in this investigation was selected based on Hasan et al. (2021c) and Zaini et. al., (2022a). For the unconfined compression test, the samples were produce by compacting soil samples with an optimal water content of the soils obtained from the compaction test. The samples were prepared and compacted in a steel mould with dimensions of 76 mm height x 38 mm diameter with a total of five (5) samples for each sample tested for different curing (1, 7, 14 and 30 days). The preparation of the samples of the materials utilized in this study is illustrated in Fig. 2.

2.2.2 Determination of the Optimal Proportion of Soft Kaolin Clay Stabilizer

The optimal percentage of admixture utilized to alter the strength characteristics of the soft kaolin clay was examined via the unconfined compression test (UCT). Five (5) samples were remoulded with a height of 76 mm and a diameter of 38 mm with respect to the optimum moisture content (OMC) obtained from the compaction test for each different percentage of mixture of SF, ESA and lime. The soft kaolin clay samples were first treated and tested with the utilisation of 2%, 4% and 6% SF. Based on the UCT test, the highest shear strength was obtained when kaolin clay was treated with 6% SF with a shear strength value of 15.51 kN/m^2. Then, 6% of the SF was selected as the optimal stabiliser of SF to be mixed with the other materials. Soft kaolin clay was further enhanced by using 6% SF with the utilization of 3%, 6%, and 9% ESA and L. At this stage, the strength of kaolin clay was observed by utilising different percentage of ESA and L to determine which material leads to the higher enhancement of strength. Based on the results obtained, the percentage of ESA and L mixture that contributed to the greatest improvement in the shear strength of soft kaolin clay mixed with 6% SF was found to be 6% and 9% with a shear strength value of 26.24 kN/m^2 and 27.38 kN/m^2. Lastly, due to the maximum strength improvement of ESA recorded at 6% of utilization, and further increment in ESA content lead to the reduction of strength, the ESA was fixed at 6% and mixed with 6% SF and were further enhanced by utilising 3%, 6% and 9% L to alter the characteristics of the kaolinitic soil.

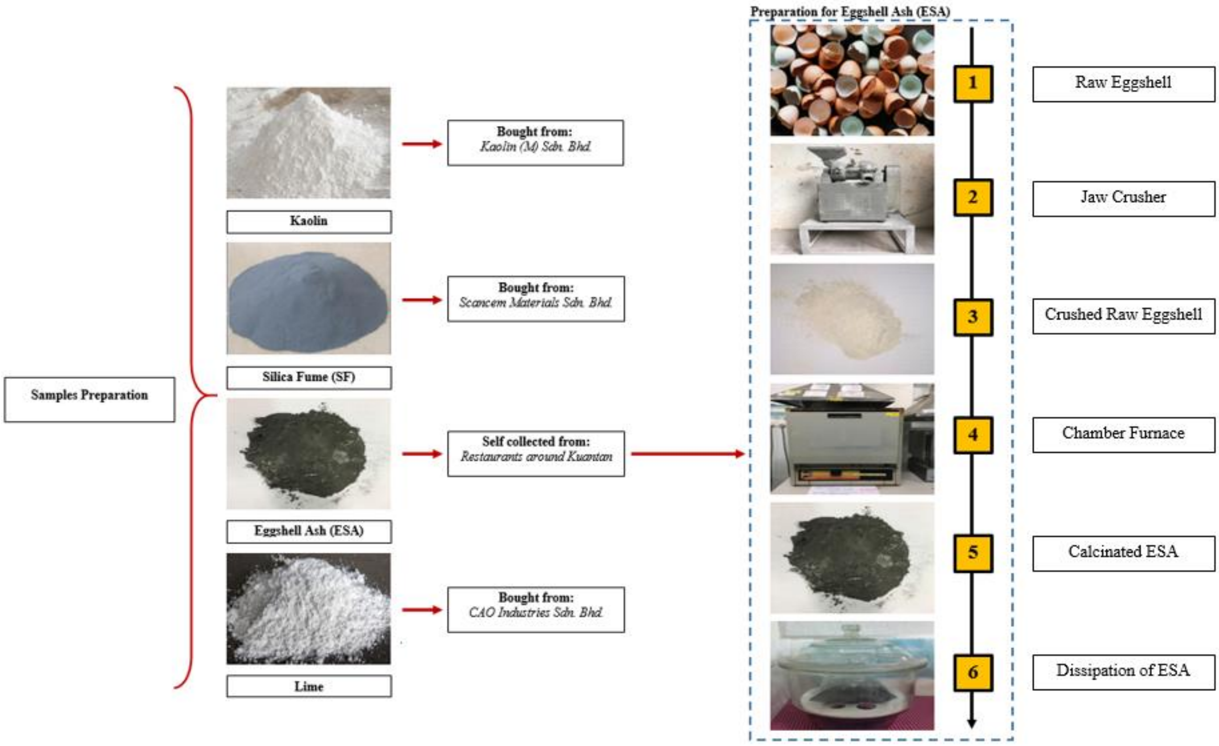

Fig. 2 - Preparation of Kaolin, Silica Fume, Eggshell Ash and Lime

2.2.3 Determination of Physical Properties of Materials

Atterberg limit and specific gravity are the physical properties examined in this study. The plasticity range of clay soil can be quantify numerically with Atterberg limits. Kaolin clay soil tend to materialise in four (4) states: solid, semi-solid, plastic, and liquid depending on a certain moisture content. Using cone penetration methods, liquid limit tests and plastic limit test were performed in accordance with BS 1377: Part 2: 1990. The term plasticity index is derived from the numerical subtraction between the liquid and plastic limits.

Small-scale pycnometer test was utilised to determine the specific gravity of the treated and untreated soft kaolin clay. Soft kaolin clay were placed in a small pycnometer bottle, with half of the bottle are already filled with distilled water and was then placed in a vacuum room for one (1) day. The vacuum chamber was used to remove air in the sample containing distilled water and the mixture of the material. Lastly, the mass of the pycnometer was measured. Specific gravity is calculated using Eq. (1).

$$Gs = \frac{m_2 - m_1}{(m_4 - m_1) - (m_3 - m_2)} \qquad (1)$$

Where m_1 is the mass of the empty pycnometer, m_2 is the mass of the pycnometer with dry soil, m_3 is the mass of the pycnometer with soil and water, m_4 is the mass of the pycnometer and water and G_s is the specific gravity.

2.2.4 Determination of Mechanical Properties of the Materials

The mechanical properties of the materials used in this study are examined via standard compaction test. Through this test, the optimal moisture content (OMC) and the maximum dry density (MDD) for treated and untreated soft kaolin clay was determined according to BS 1377-2:1990. Three (3) layers were compacted by a free fall hammer method with 25 blows per layer. The OMC and MDD were determined from the graph plotted between the dry unit weights against the moisture content.

2.2.5 Determination of the Undrained Shear Strength of the Materials

The undrained shear strength of treated and untreated kaolin clay was examined using UCT tests. The density of treated and nontreated soft clay was 1.74 kg/cm^3. The density of both samples is consistently preserved in the UCT tests because the data must be sustained for their consistency. The UCT was performed according to ASTM E1621-16 to determine the strength of the soil. In this test, the data on the axial load of the failure and the corresponding axial stress were recorded together with the failure mode pattern. Tests were carried out with 2%, 4%, 6% SF; 6% SF with 3%, 6%, and 9% of ESA and L; 6% SF and 6% ESA with 3%, 6% and 9% of L for treated samples at different duration of curing durations (1 day, 7 days, 14 days and 30 days). Control samples are used without SF, ESA, and L mixtures. A total of 260 UCT were performed on kaolin clay samples, as the tests were carried out on 13 set of samples (13) each with five (5) samples for four (4) different curing durations. The result of the undrained shear strength was half of the unconfined compression strength. Solid soil shear resistance (S_u) is equal to half the unconfined compressive resistance (q_u), as shown in Eq. (2).

$$S_u = c = \frac{q_u}{2} \qquad (2)$$

In which Su is the undrained shear strength, c is the cohesion, and qu is the unconfined compressive strength.

2.2.6 Determination of Chemical Oxide Compositions of Materials

The chemical oxide composition of kaolin, SF, ESA, lime and kaolin admixed with various percentages of SF, ESA and L was tested using a Bruker S8 Tiger X-ray Fluorescence (XRF) analyzer and fully compliant to ASTM E1621-13. For this test, 10 g of each of the samples were gathered and stored in an airtight plastic bag before being dispatched to the laboratory for testing. The analysis was crucial in determining the suitability of the SF, ESA and L based on the chemical oxide compositions as stabilising agents in soft kaolin clay.

2.2.7 Determination of Mineralogical Characteristics of the Materials

The mineral and crystallography of kaolin, SF, ESA , L and kaolin mixed with various percentages of SF, ESA and L was analysed using the Bruker D8 Advance Diffractometer at the position 2-theta (2θ) position with ASTM D3906-19. 10 g of each sample were gathered and retained in an airtight ductile bag before being sent to the laboratory. XRD analysis is very important to complement with XRF analysis conducted. XRD allows examination of the phases in crystalline substances, which further examines the composition of the substances and gives information on the calcium oxide (CaO), calcium carbonate ($CaCO_3$), calcium hydroxide ($Ca(OH)_2$) constituents and other calcium (Ca) phases or iron (Fe) phases, such as iron oxide (FeO), iron trioxide (Fe_2O_3), iron oxide black (Fe_3O_4), iron carbide (Fe_3C) and other iron (Fe) phases. Consequently, compounding the results of both the mineralogical and chemical oxide composition approaches permits a finer and more absolute delineation of any given crystalline specimen.

2.2.8 Determination of Morphological Characteristics of the Materials

The sieve analysis was performed in accordance with BS 1377: 2: 1990 and the hydrometer analysis was performed in accordance with ASTM D422. The grain size distribution of fine soil, was determined by performing the hydrometer test. Besides, the sieves used to analyse the particle sizes of the untreated and treated soft kaolin clay were 20 mm, 10 mm, 4.75 mm, 2.36 mm, 1.18 mm 0.6 mm, 0.3 mm, 0.15 mm, and 0.063 mm. The sieves were stacked together with the largest opening size at the top and the pan under the smallest opening of the sieves at the bottom. The sieving process was performed using a mechanical shaker and the proportions of soil left on each sieve were measured using the mass balance. A distribution curve was then plotted with the percentage of particles retained in each sieve. The sieve analysis can be carried out under either wet or dry conditions. In this research, dry sieve analysis was selected. The percentage passing versus the particle size results were plotted in the semi-logarithmic graph. The results of the treated and untreated soft kaolin clay were utilised to determine the similarity of the soil material with the group in the classification system.

2.2.9 Determination of Microstructural Characteristics of Materials

To characterise the surface texture, particle shape and angularity of the materials, kaolin, SF, ESA, L, and treated soft kaolin clay with various percentages of SF, ESA, and L were subjected to microscopic examination that was performed using the Field Emission Scanning Electron Microscope (FESEM) model ZEISS EVO 50. By rastering a focused electron beam across the surface and detecting backscattered or secondary electron signals, FESEM produces detailed high-resolution images of the sample. Also, the images were captured on photomicrographs in addition to digitalising the files.

3. Results and Discussion

3.1 Physical Properties of Treated and Untreated Soft Kaolin Clay

Fig. 3 presents the specific gravity of four (4) different types of soft kaolin clay treatment compared to the untreated kaolin clay and SF, ESA and L. Based on Fig. 3(a), the specific gravity of the soft kaolin clay when treated with 2%, 4% and 6% of SF is significantly higher than the raw SF with a different margin (MD) of 0.21, 0.18 and 0.17

while slightly lower than the untreated kaolin clay with an MD of 0.10, 0.13 and 0.14. Inclusion of SF in the soft kaolin clay treatment leads to the reduction of the specific gravity of the soft kaolin clay as the portion of the SF increases. Similar investigations have been revealed by Zaini et al. (2022a) for the utilization of SF in the soft kaolin clay treatment. Furthermore, similar trending was observed when the soft kaolin clay was treated with different ESA, L and the combination of ESA-L (see Fig. 3(b) to Fig. 3(d)). The higher the ratio of soil stabilizer used in the treatment of the soft kaolin clay leads to the higher reduction of the specific gravity. The highest reduction in specific gravity was observed when soft kaolin clay was treated with the combination of 6% SF, 6% of ESA and various percentages of L (K6SF6ESA3L, K6SF6ESA6L, and K6SF6ESA9L) with a specific gravity value of 2.51 (4.92% reduction), 2.45 (7.20% reduction) and 2.38 (9.85% reduction). The reduction of specific gravity was almost identical when the soft kaolin clay is treated with various percentages of ESA (K6SF3ESA, K6SF6ESA, and K6SF9ESA) and L (K6SF3L, K6SF6L, and K6SF9L) with a reduction of 1.52%, 3.79%, and 4.92% for the use of ESA and a reduction of 0.76%, 3.41%, and 4.55% for the utilization of L.

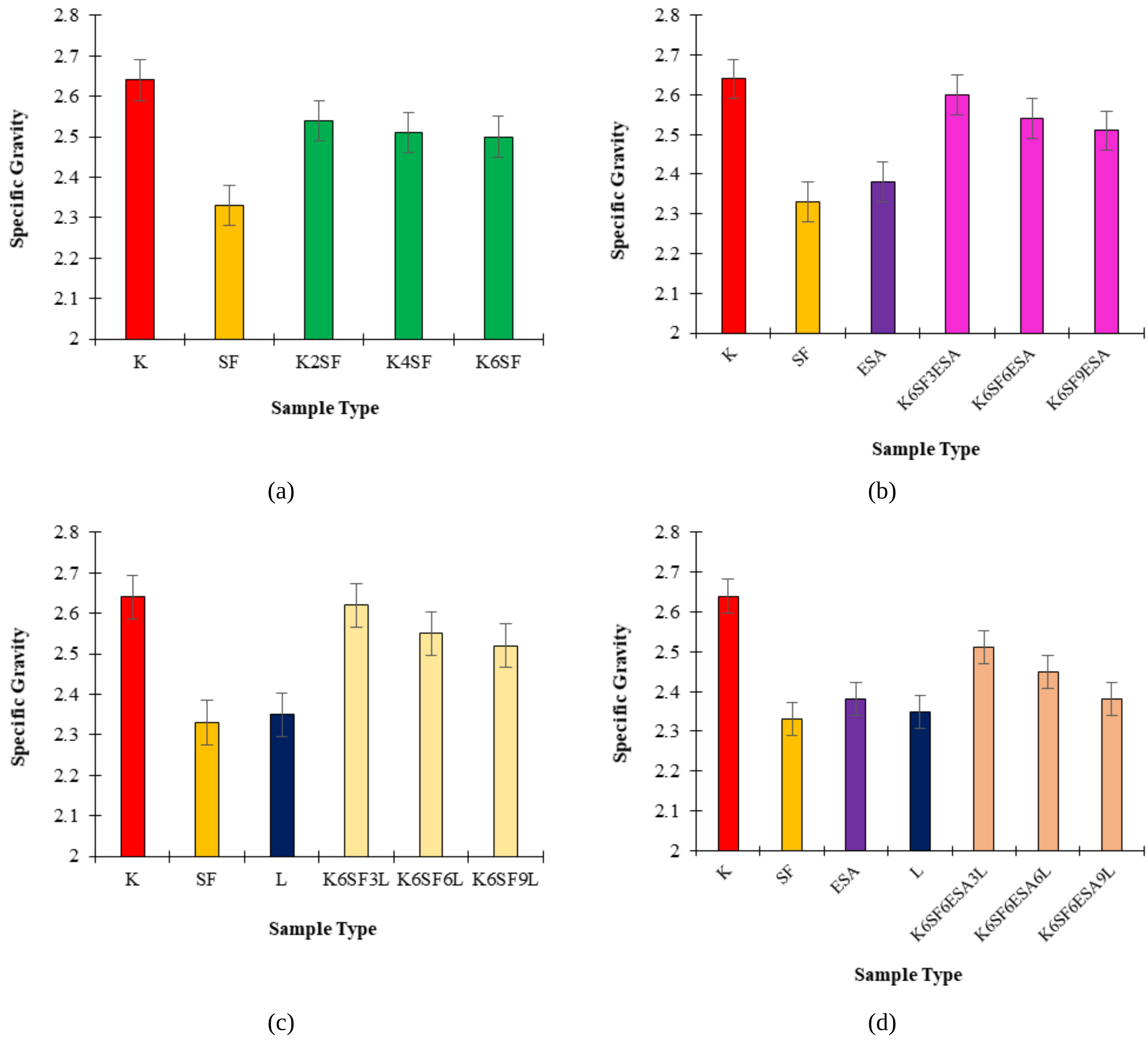

Fig. 3 - Effect of different ratio of: a) SF; b) SF-ESA; c) SF-L and; d) SF-ESA-L to the specific gravity of the soft clay treatment. SF, Silica Fume; ESA, Eggshell Ash; L, Lime; 2, 3, 4, 6 and 9, percentage of stabilizer utilized in the soft kaolin clay treatment

Fig. 4 illustrates the general specific gravity of untreated kaolin, SF, ESA, L and treated kaolin using different combination percentages of SF (2%, 4%, and 6%), combination of SF-ESA (SF = 6%; ESA = 3%, 6% and 9%), combination of SF-L (SF = 6%; L = 3%, 6% and 9%) and combination of SF-ESA-L (SF = 6%; ESA = 6%; L = 3%, 6% and 9%). Based on Fig. 4, the observation shows that when the soft kaolin clay was treated with SF, ESA and L, the specific gravity was reduced as the particles became less denser due to restructuring of the soil matrix as lighter SF, ESA (Hasan et al., 2021c) and L (Chemeda et al., 2018) are added to the soft kaolin clay, thus forming a lighter soil mixture. As the specific gravity of SF, ESA, and L is smaller than the specific gravity of soft kaolin clay, the findings proved that by using SF, ESA and L as the soil stabiliser, the specific gravity of the soft kaolin clay can be altered from denser soil particles to lighter soil particles. The combination of SF, ESA, and L in soft kaolin clay resulted in the largest reduction in specific gravity followed by the combinations of SF-L, SF-ESA, and SF alone. Similar situations were assessed in the investigation performed by Zaini et. al., (2022a) and Türköz et. al., (2021). Therefore, it can be proven that the utilisation of SF, ESA, and L can alter the physical properties of the soft kaolin clay in terms of specific gravity.

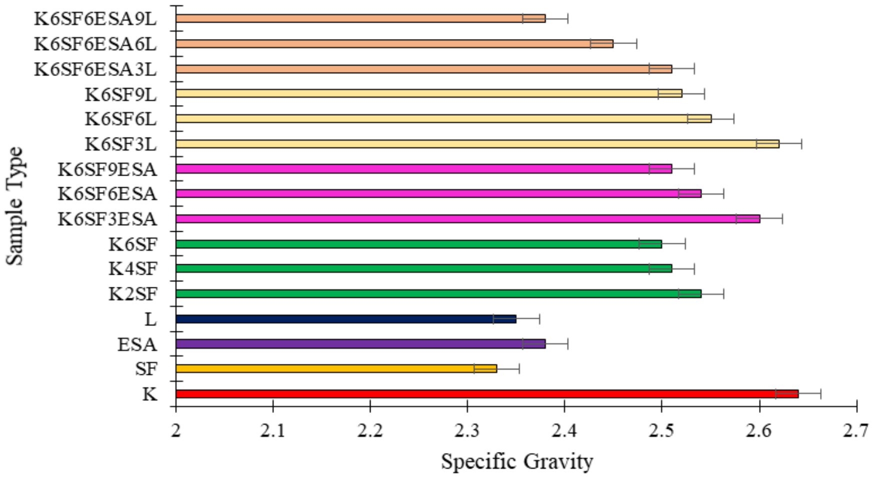

Fig. 4 - The general comparison of specific gravity between untreated soft kaolin clay with the raw stabiliser material and the treated soft kaolin clay. SF, Silica Fume; ESA, Eggshell Ash; L, Lime; 2, 3, 4, 6 and 9, percentage of stabilizer utilised in the soft kaolin clay treatment

The Atterberg limits are the key variable that assists in delineating the plastic nature of the soft kaolin clay. Atterberg limits tests were carried out after two (2) days of addition to assess the effect of SF, ESA and L on the kaolin clay soil consistency limits. Significant alteration takes place in the Atterberg limits with the addition of SF, ESA, and L. The results of the PL, LL and PI of the untreated kaolin and treated kaolin samples with various ratios of SF, combination of SF-ESA, combination of SF-L and combination of SF-ESA-L have been demonstrated in Figs. 5(a) to 5(d) together with the penetration graph for LL validation of the optimum stabilizer sample (K6SF, K6SF6ESA, K6SF9L and K6SF6ESA9L) for the optimum utilization of the SF, combination of SF-ESA, combination of SF-L and combination of SF-ESA-L. Based on Fig. 5(a), the use of SF slightly decreases the PL and LL of the soft kaolin clay at 2% and 4% from 33.3% to 29.8% and 31.6%; from 40.9% to 37.1% and 38.4% while further inclusion of SF at 6% increases PL and LL up to 34.5% and 41.1% with an MD of 1.2% and 0.2% . The PI of the SF treated kaolin sample continuously decreases at 2%, 4% and 6% from 7.6% to 7.3%, 6.8% and 6.6%. Therefore, the PI of the treated soft kaolin clay was diminished with respect to increases in the SF content, resulting in an increase in soil workability. There were continuous increases in PL with an increase in the SF content at 6% of use, a reaction that may be owing to the cation interchange that takes place between clay minerals of kaolin and positive cations in SF (Türköz et al., 2021). The increase in LL at 6% of SF was due to an expansion of disperse dual layer (articulation related to hovering cations and a small amount of anions around kaolin clay molecules) created by an increase in the particular surface area which then increases the water retention capacity of the soft kaolin clay. The depletion in plasticity characteristics of the soft kaolin clay can be ascribed to the substitution of highly plastic clay molecules with non-amiable SF molecules. Furthermore, the inclusion of SF in soft clay soils causes flocculation, thus diminishing the plasticity index. Identical scenarios have been investigated by Hasan et al. (2021c) and Türköz et al., (2021).

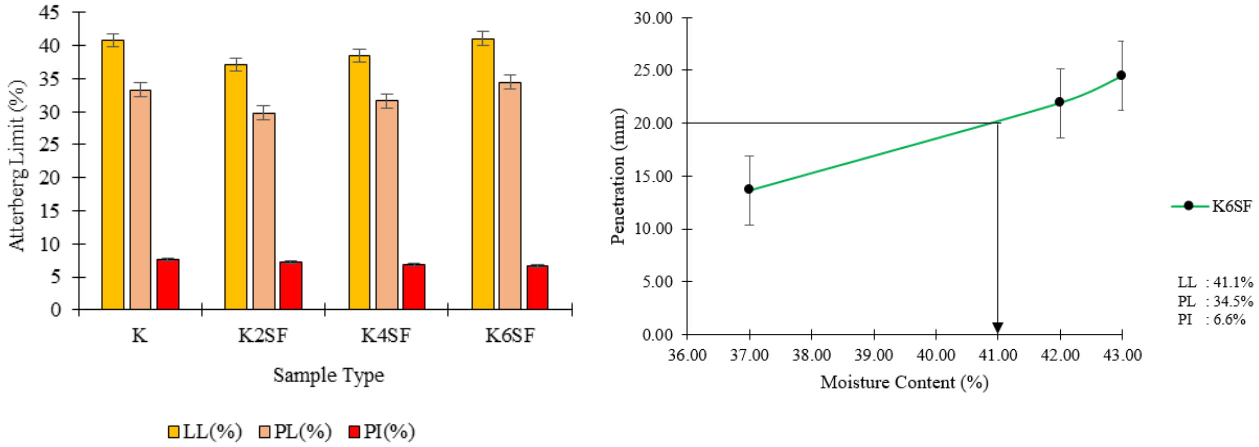
Atterberg Limit (%)
K
K2SF
K4SF
K6SF
Sample Type
LL(%) PL(%) PI(%)
Penetration (mm)
Moisture Content (%)
K6SF
LL : 41.1%
PL : 34.5%
PI : 6.6%

(a)

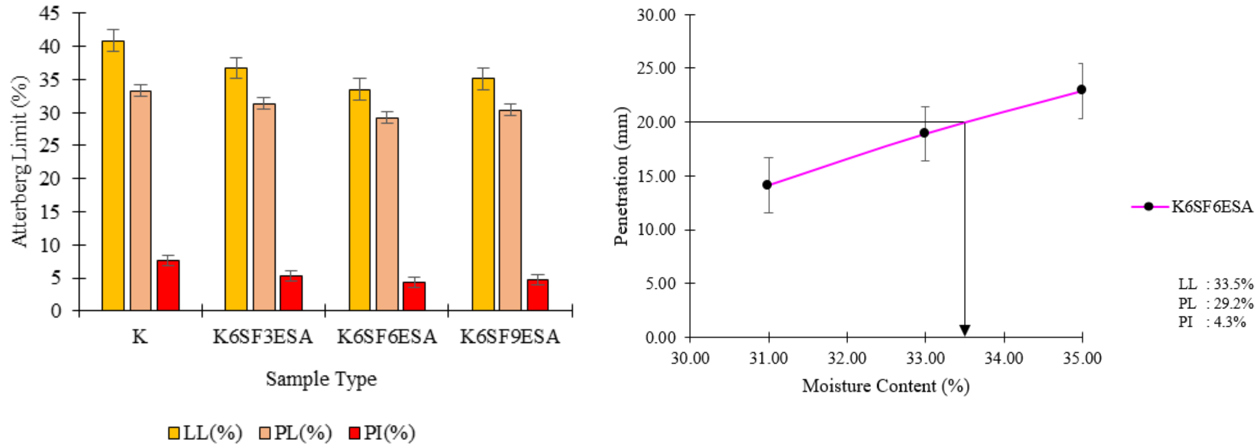
Atterberg Limit (%)
K
K6SF3ESA
K6SF6ESA
K6SF9ESA
Sample Type
LL(%) PL(%) PI(%)
Penetration (mm)
Moisture Content (%)
K6SF6ESA
LL : 33.5%
PL : 29.2%
PI : 4.3%

(b)

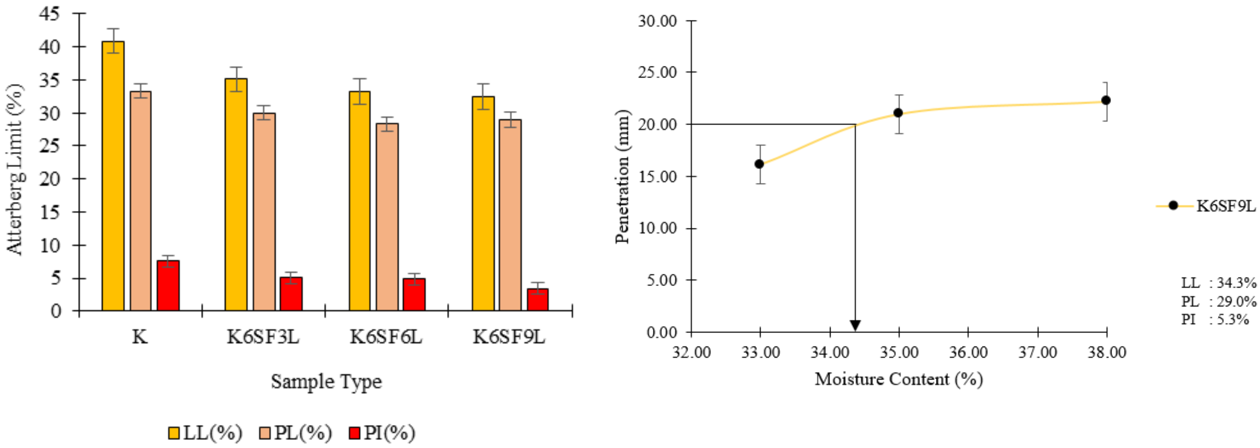
Atterberg Limit (%)
K
K6SF3L
K6SF6L
K6SF9L
Sample Type
LL(%) PL(%) PI(%)
Penetration (mm)
Moisture Content (%)
K6SF9L
LL : 34.3%
PL : 29.0%
PI : 5.3%

(c)

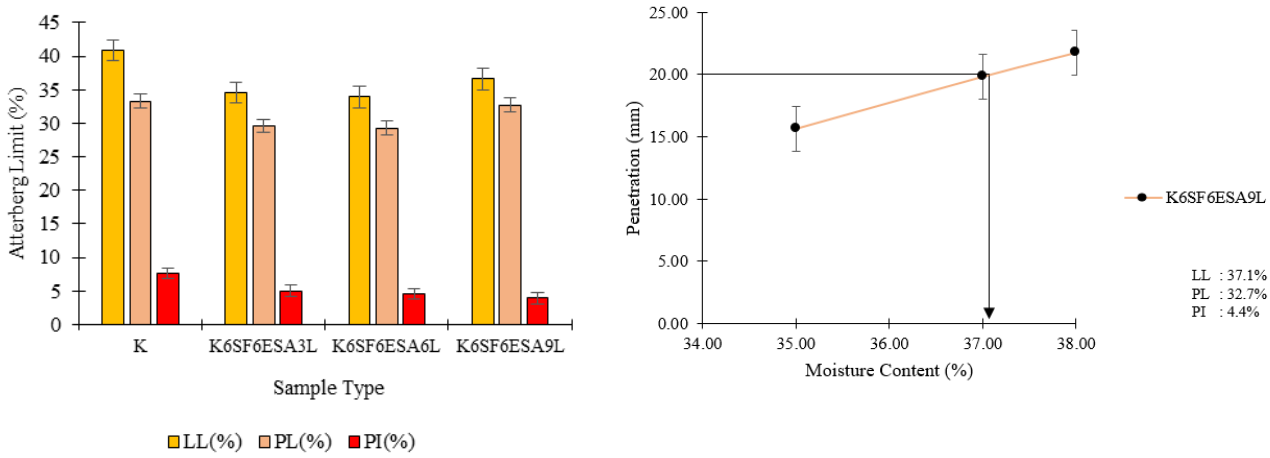

(d)

Fig. 5 - Effect of different ratios of: a) SF; b) SF-ESA; c) SF-L and; d) SF-ESA-L to the consistency limits of soft kaolin clay treatment. SF, Silica Fume; ESA, Eggshell Ash; L, Lime; 2, 3, 4, 6 and 9, percentage of stabilizer utilised in the soft kaolin clay treatment

The chemical compositions of ESA and L are almost identical, the SiO2 content and CaO content in L are slightly higher than that of ESA. Therefore, based on Fig. 5(b) and Fig. 5(c) the pattern of the graph is almost identical as the PL and LL of the soft kaolin clay treated with ESA and L were reduced from 33.3% to 31.4%, 29.2%, 30.4% and 30.0%, 28.3%, 29.0% as the ratio of ESA and L inclusion increases. Regarding PI, the higher ratio of L of ESA and the inclusion ratio resulted in a lower value of PI of soft kaolin clay with an MD of 2.3%, 3.3%, 2.9% and 2.5%, 2.7%, 4.2%. Furthermore, the combination of SF-ESA-L (see Fig. 5(d)) resulted in a higher content of SiO2 and CaO, leading to the larger surface area and greater molecule bonding of the treated soft kaolin clay. Thus, PL and LL are significantly reduced together with PI. As stated by Türköz et al. (2021), there was a reduction in PL with increases in L content in a constant ratio of SF and ESA at 6% of utilisation, a reaction that may be owing to the cation exchange that occurs between the kaolin clay minerals and calcium ions in ESA and L. The depletion in the water retention volume can be ascribed to molecules of stabilizers that varnish the kaolin clay molecules, cohere them together, and finally, permeate the kaolin clay matrix. Thus, this resulted in the depletion of voids and the water accommodated within these voids.

The treated soft kaolin clay becomes more levigated owing to the coagulation and accumulation reaction, which exhibit a silt-like quality to the kaolin clay molecules. Kaolin clay molecules take place owing to the substitution of monovalent ions by Ca^{2+}. This results in depletion of plasticity, which intensifies the workability. The increase in the liquid limit and plastic limit of kaolin clay in the inclusion of L can be ascribed to the increment in the affinity of kaolin clay molecules for water. Therefore, it can be recommended that both ESA and L can cohere and coagulate the kaolin clay to be rough, with a depletion of the fine clay content through the cation exchange activity and pozzolanic reactions. These results are identical to the past investigations conducted by Zaini et al. (2022a). All the penetration graph proved that the manual calculation of the LL obtained in this study is accurate and precise, as the LL obtained from the manual calculation is identical to the plotted penetration graph of LL. Fig. 5 proved that the use of SF, ESA and L can change the physical characteristics of the soft kaolin clay in terms of consistency limit.

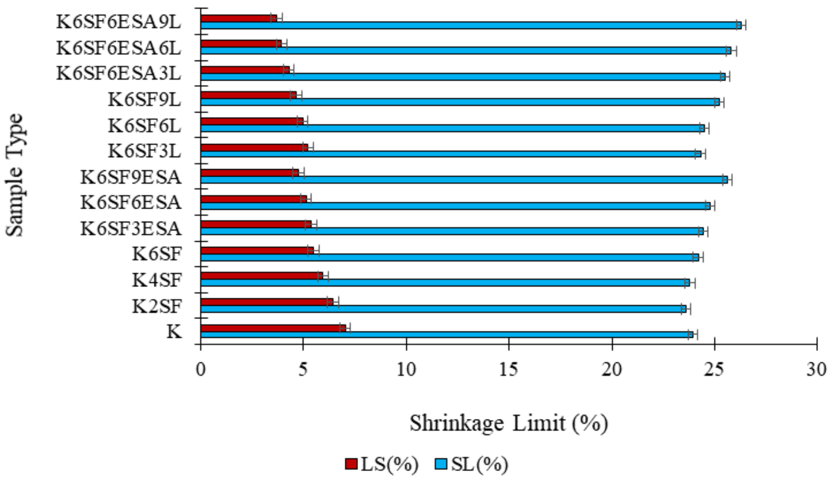

Fig. 6 - Effect of different ratios of: a) SF; b) SF-ESA; c) SF-L and; d) SF-ESA-L to the shrinkage limit and linear shrinkage of soft kaolin clay treatment. SF, Silica Fume; ESA, Eggshell Ash; L, Lime; 2, 3, 4, 6 and 9, percentage of stabilizer utilized in soft kaolin clay treatment

Fig. 6 illustrates the SL and LS of treated and untreated soft kaolin clay at various percentages of inclusion of SF, ESA, and L. Through the drying process of the soft kaolin clay, the kaolin clay molecules appear to be in proximity with each other; whereby a further decrease in moisture does not alter the volume of the soft kaolin clay mass as the soft kaolin clay acts as a solid. The water content in this phase is known as SL, which quantifiably dominates the tendency of the soft clay soil to dwindle. Generally, the lower the SL leads to the higher shrinkage capacity. Based on Fig. 6, the SL of soft kaolin clay treated with 2% SF slightly reduced SL and LS from 23.93% to 23.61% and from 7.02% to 6.43% with an MD of 0.32% and 0.59% due to the replacement of SF in the 2% portion of the soft kaolin clay. However, the SL of soft kaolin clay consistently increases with the increment ratio of SF, SF-ESA, SF-L and SF-ESA-L with the highest recorded SL of 26.31% with an MD of 2.38% while the LS consistently decreases with the highest reduction of 3.69% with an MD of 3.33%. The rise in SL is ascribed to the accumulation of molecules due to the alteration of ESA and L. The soft kaolin soil, being tremendously plastic, was originally in diffused condition. With the increase in molarity absorption owing to the alteration of ESA and L, the thickness of the duplex layer decreases and the repulsion between the kaolin clay molecules decreases, resulting in the formation of aggregated conglomeration. These aggregated conglomerations raised resistance against capillary intake influenced by volumetric shrinkage directing to an increase in shrinkage void ratio and via the water content. However, in soft kaolin clay, the SL does not affect much of the modification in the SL, but is only significantly affected via LS. For such an exposition, the composition of the ESA-L treated kaolin clay soils has persisted substantially in the aggregation area.

The highest SF-ESA-L replacement in soft kaolin clay leads to a highly open structure that holds a substantial volume of water onto the molecules (Dash & Hussain, 2015), thus increasing LL. In addition, the treated soft kaolin clay has a well-constructed structure that functionally repels contraction, thus increasing the SL. The current soft clay soil is predominantly non-swelling kaolinitic, which contains a lesser fines contentment, and the domination of disseminate duplex layer recession with the microscopic amount of ESA and L is insignificant. Preferably, the ESA-L persuaded lubrication has promoted intergranular repositioning during contraction resulting in preferable formation and thus decreased SL. However, the increase in ESA and L in the treatment of soft kaolin clay led to a significant increment in LL and SL ascribed to the emergence of a calcium silicate hydrate gel that withstands the substantial amount of water onto it. The results obtained agree well with previous researchers on soil-lime fusion (Dash & Hussain, 2015; Hasan et al., 2021c).

3.2 Mechanical Properties of Treated and Untreated Soft Kaolin Clay

The relationship between MDD and OMC of soft kaolin clay treated with various ratios of SF, ESA, and L is illustrated in Fig. 7. The MDD for untreated soft kaolin clay was 1.55 g/cm^3, with an OMC of 21%, which is in the range of values stated by Blayi et al., (2020) and Bozyigit et al., (2021). Based on Fig. 7, when soft kaolin clay was treated with 2%, 4% and 6% SF, the reduction of MDD and OMC was initiated in the K2SF sample with MDD and OMC of 0.04 g/cm3 and 3.0%, then gradually increases in MDD when 4% and 6% of SF were utilized with MDD of 1.51 g/cm^3 and 1.52 g/cm^3 while OMC constantly decreases to 17.5% and 17.9%. The increase in OMC was proportionally restricted. Suppose that the lower value of specific gravity and the coarser particle sizes of the SF resulted in the additional void volume developed. Consequently, the thickness of the duplex layer will decrease and produced grain accumulation will be produced due to the substitution of sodium cations in the diffusive clay of soft kaolin clay with silicon cations (Türköz et al. 2021). However, the result obtained was not in good agreement with the investigation conducted by Türköz et al. (2021) in terms of particle size, which shows that the utilisation of the 2%, 4% and 6% of SF does diminish the specific gravity of the soft kaolin clay, but do not significantly affect the particle size of the soft kaolin clay, resulting in the slight reduction of OMC in the various utilisation ratio of SF. The scenario was due to the insignificant substitution of SF that replaced soft kaolin clay particles in the treatment. Moreover, the dominant Silty-type soil exists in the soft kaolin clay leaded to closely packed molecules, preventing the additional void volume to occur. Therefore, it resulted in a reduction of OMC when the untreated kaolin samples were treated with 2%, 4% and 6% SF.

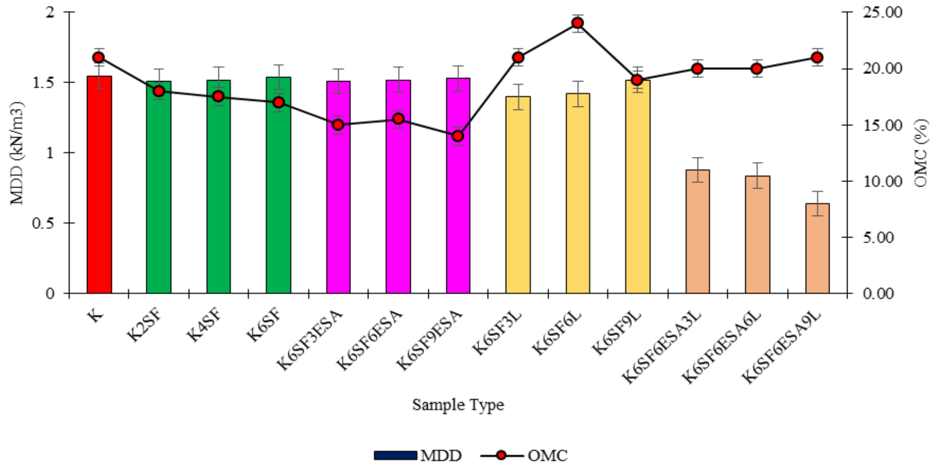

Fig. 7 - Relationship between OMC (%) and MDD (kN/m^3) of the untreated and treated soft kaolin clay

At optimum utilization of 6% of SF, soft kaolin clay was further treated with 3%, 6% and 9% of ESA and L individually and in combinations of ESA-L, resulting in a significant reduction in MDD with a MDD value of 1.51 g/cm^3, 1.52 g/cm^3, 1.53 g/cm^3; 1.40 g/cm^3, 1.42 g/cm^3, 1.52 g/cm^3 and 0.88 g/cm^3, 0.84 g/cm^3 and 0.64 g/cm^3 from 1.55 g/cm^3 of the untreated soft kaolin clay. Depletion in MDD can be ascribed to the hydration, dissociation, and pozzolanic reactions that lower the density of the SF-ESA and SF-L mixtures individually or in combinations of SF-ESA-L. Nevertheless, the molecules organization of the soft kaolin clay was closely packed together when the ESA and L were added to the soil sample, hence altering the specific area of the soft kaolin clay. Owing to the specific area alterations, water absorption is needed for the chemical reaction to take place among the fine molecules to embark on the improvement process of the soft kaolin clay. The removal of the MDD is reliable on the OMC. Therefore, the OMC of the treated sample undergoes fluctuation owing to the adsorption capacity of ESA and L, ascribable to the porosity characteristics, and the increased OMC with an increasing ratio of ESA and L up to 6% and 9%, respectively. This phenomenon was affected by the increase in CaO content in the treated sample, so a large quantity of water is required (Jafer et al., 2018) for the emergence of CSH molecules and the pozzolanic reaction with the existence of SF. The pattern of the graph is in line with the study performed by (Zaini et al., 2022a; 45]. Therefore, it can be deduced that the combination of SF-ESA, SF-L, and SF-ESA-L can reduce the bulging propensity of the soft kaolin clay. The obscurity to generate consistency limits in the Atterberg limit test ensued to the ill-suited compaction test to be executed for the SF, ESA, and L. Therefore, the compaction test for SF, ESA and L was omitted from the study.

3.3 Unconfined Compressive Strength of Soft Kaolin Clay at Various Curing Time

The UCS of the untreated kaolin clay and treated kaolin clay with various ratios of SF, ESA, and L at various curing times are demonstrated in Fig. 8(a) to Fig. 8(d) and Fig. 9 shows the strength improvement of treated soft kaolin clay with various ratios of SF, ESA, and L at different curing times. Initially, the soft kaolin clay was treated with 2%, 4%, and 6% SF at various curing times of 1 day, 7 days,, 14 days and 30 days. Based on Fig. 8(a), the result urges that the compressive strength of the soft kaolin clay rise gradually when 2% of the SF is mixed with the soft kaolin clay from 13.154 kN/m^2 to 13.794 kN/m^2 (1 day of curing), 16.534 kN/m^2 (7 days of curing), 18.238 kN/m^2 (14 days of curing) and 18.664 kN/m^2 (30 days of curing) with a strength improvement of 4.64%, 20.30%, 26.08% and 25.55%, respectively, and reached its optimal strength at 15.512 kN/m^2, 21.844 kN/m^2, 23.058 kN/m^2 and 24.530 kN/m^2 when 6% of SF was utilised with a strength improvement of 15.20%, 39.67%, 41.53% and 43.35% on different days of curing. The enhancement of soil strength was due to the sufficient amount of amorphous silica and alumina in SF that lead to the pozzolanic reactivity of the soil. Similar observations have been reported by Zaini et. al., (2022a) and Mahmutluoğlu and Bağrıaçık (2022) without considering the curing time. Furthermore, 6% of SF usage is maintained for the next improvement in the strength of soft kaolin clay.

The hydration process of ESA and L will yield the production of CaO which is an ideal material to utilise with SF as cementitious materials. However, the performance of these two (2) materials in enhancing the strength of the kaolin clay should be investigated and compared. Therefore, at this stage, ESA (see Fig. 8(b)) and L (see Fig. 8(c)) were tested differently with the use of SF as to assess which material contributed to a higher strength improvement. The results suggested that the utilisation of the ESA at the optimal percentage of 6% at different curing times (49.87%, 49.90%, 49.57% and 49.78% of strength improvement) exceeds the use of L at 3% (38.33%, 47.59%, 49.10% and 51.58% of strength improvement) but does not exceed the optimal utilisation of L at 9% (51.95%, 69.41%, 73.21% and 80.22% of strength improvement) with a margin difference of 1.136 kN/m^2. Based on the results obtained, both stabilisers (ESA and L) can be used as a soil stabilising agent, as both materials enhance the strength of soft kaolin clay on different curing days from 13.154 kN/m^2 to 26.24 kN/m^2, 26.306 kN/m^2, 26.374 kN/m^2, 27.670 kN/m^2; and 27.376 kN/m^2, 43.078 kN/m^2, 50.324 kN/m^2 and 70.242 kN/m^2 respectively. However, the performance of L in soil improvement is slightly better than ESA, as demonstrated in Fig. 9.

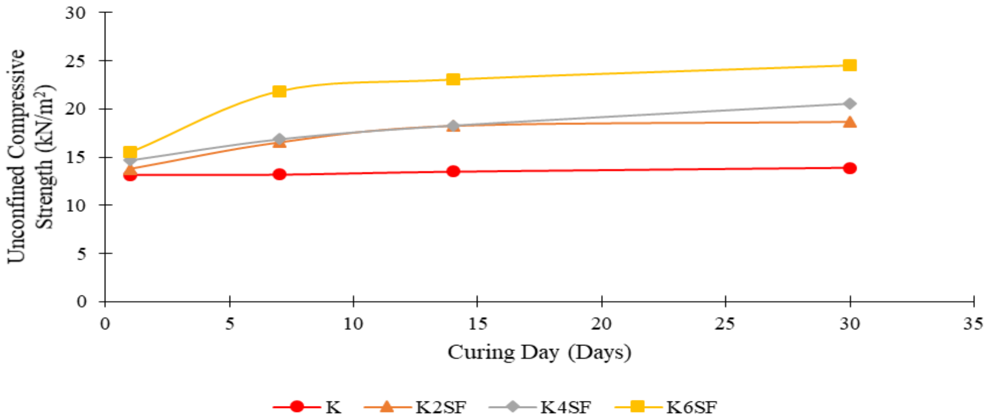

(a)

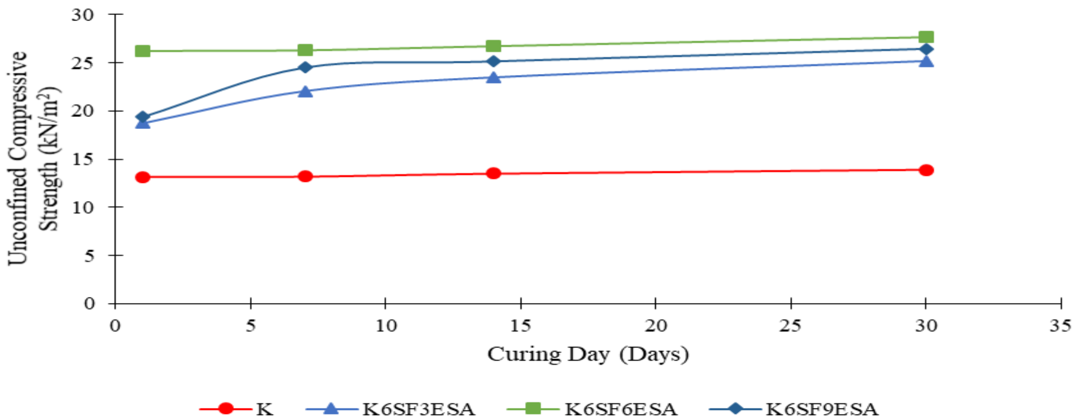

(b)

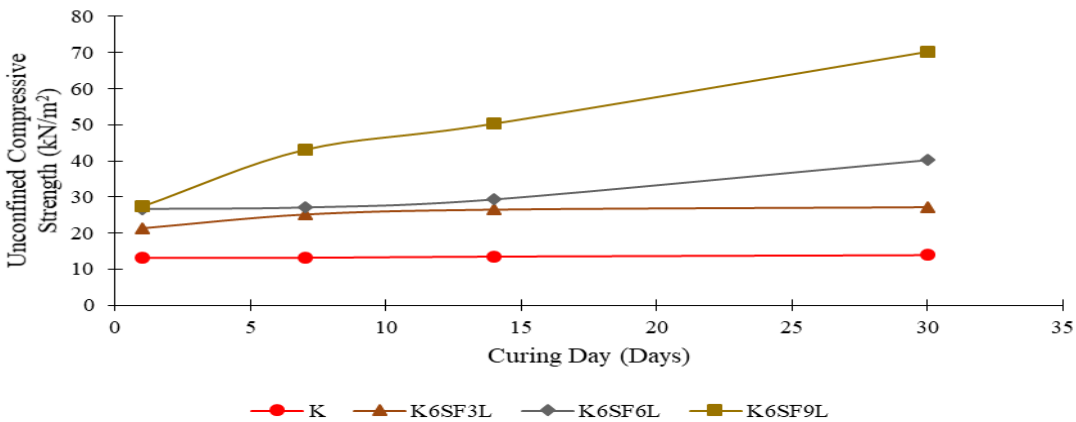

(c)

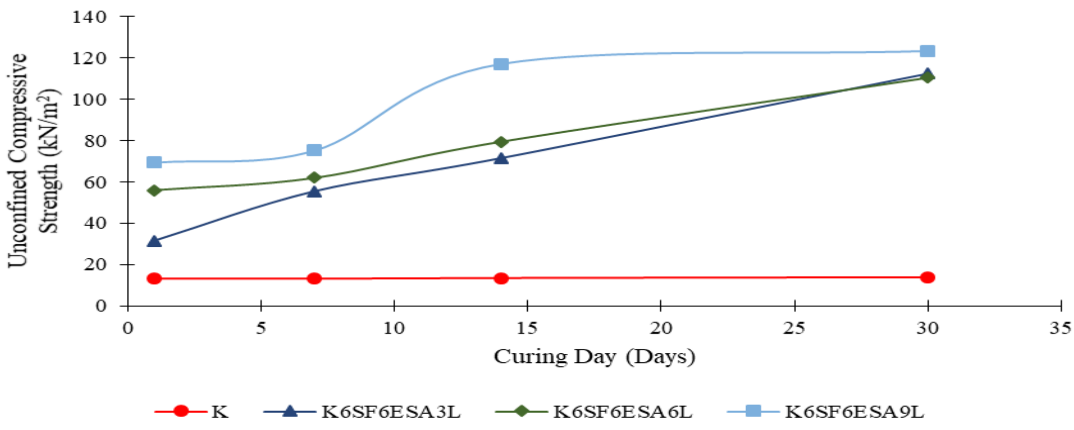

(d)

Fig. 8 - Effect of a different ratio of: a) SF; b) SF-ESA; c) SF-L; d) SF-ESA-L to the unconfined compressive strength of soft kaolin clay at 1 day, 7 days, 14 days and 30 days of curing

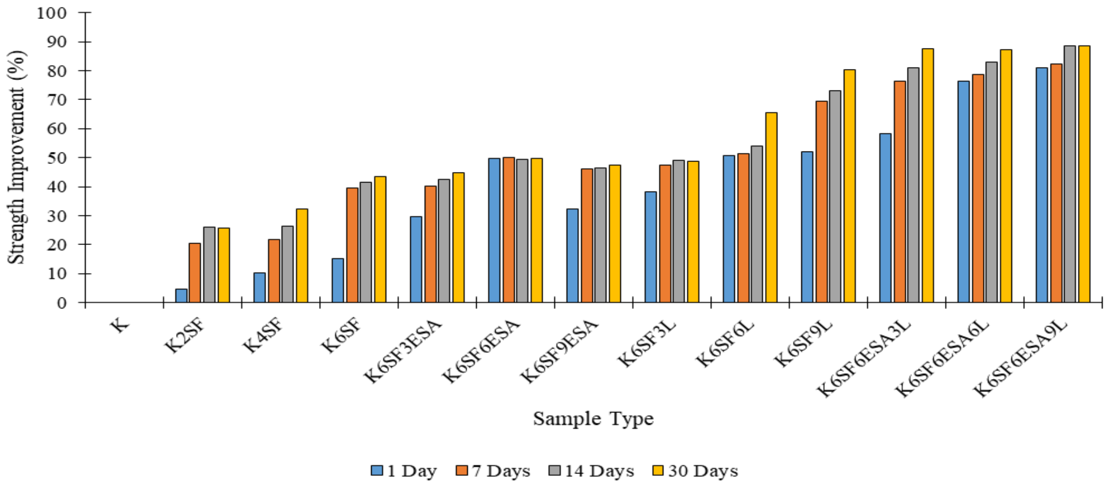

Fig. 9 - Strength Improvement of treated soft kaolin clay with various ratio of SF, ESA, L at different curing time

Furthermore, since ESA reached the optimal strength at 6% and the additional inclusion of ESA led to the reduction of soil strength, ESA was selected as the second material to be kept constant to be used with a different ratio of L to further enhance the strength of the soft kaolin clay. The results obtained suggested that, continuous utilization of the SF-ESA-L mixture (see Fig. 8(d)) at different curing days leads to a higher UCS achievement of up to 81.03%, 82.46%, 88.49% and 88.74% of strength improvement (69.344 kN/m^2, 75.150 kN/m^2, 117.144 kN/m^2 and 123.436 kN/m^2). The utilisation of 3%, 6% and 9% of L utilised with 6% of SF and ESA exceeded the UCS value of untreated kaolin clay and treated kaolin clay with SF, SF-ESA and SF-L. Nevertheless, mechanisms, for instance, the cation exchange reaction, flocculation of kaolin clay molecules, pozzolanic reactivity, and agglomeration, are the main physiochemical reactions that regulate the engineering characteristics of kaolin-treated mixtures. Responses, for instance, dissociation and interchange of cations, help to instantaneous alterations in the workability of the soil which strengthen the link between the soil molecules and increase the strength of the soft kaolin clay. Furthermore, the curing time became an important factor in determining the maturity of the soil sample, leading to the highest improvement of the strength of the sample.

3.4 Chemical Oxide Compositions of Treated and Untreated Soft Kaolin Clay

Table 2 presents the chemical oxide compositions of soft kaolin clay alone and treated soft kaolin clay with SF, ESA and L. Pozzolanic reactivity and cementitious characterisation are the dual requisite aspects in altering the characteristics of soft kaolin clay. Like cement, ESA and L also encounter the hydration process. Several studies have been performed to determine the hydration products of ESA (Sathiparan, 2021; Sharma et al., 2018). Silicon dioxide (SiO_2) and calcium oxide (CaO) are examined as the essential element of cementitious substance with the presence of water becoming the limitation factor for both of the substances. Pozolanic reactivity is a stagnant interactivity and is responsible for altering the engineering characteristics of the soft kaolin clay that depend on two (2) aspects, which are the prominent quantify of $Ca(OH)_2$ with which pozzolan can counter and the surface area of pozzolan. With increased water during the hydration process, CaO will react with the water and institute calcium hydroxide, $Ca(OH)_2$ as demonstrated in Eq. (3).

Hydration reaction:

$$CaO + H_2O \xrightarrow{Hydration} Ca(OH)_2 \quad (3)$$

Nevertheless, the dissociation reactions open up to instantaneous alteration in the pliability and workability of the soft kaolin clay, as highlighted in the Eq. (4). For instance, cation interchange, emulsification of soft kaolin clay molecules, accumulation, and pozzolanic processes are the predominant physicochemical responses that affect the characterisation of Kaolin-SF-ESA-L mixtures. Ca^{2+} of the ESA and L that exist in the treated kaolin clay retaliate against the existence of water by obeying the chemical reaction path stated in the Eq. (5) and Eq. (6).

Dissociation Reaction:

$$Ca(OH)_2 \longrightarrow Ca^{2+} + 2OH^- \quad (4)$$

Pozzolanic reaction:

$$Ca(OH)_2 + SiO_2 \longrightarrow CSH \quad (5)$$

$$Ca(OH)_2 + Al_2O_3 \longrightarrow CAH \quad (6)$$

Table 2 - The main chemical content of the untreated kaolin and the treated kaolin with SF-ESA-L were determined by XRF

Sample Type	Compositions (%)					
	SiO_2	CaO	Al_2O_3	K_2O	MgO	Fe_2O_3
K	66.11	0.08	19.25	2.85	1.23	0.73
SF	74.02	0	0.45	4.27	3.73	0.71
ESA	0.02	62.5	0.01	0.05	0.71	0.02
L	1.4	72.6	0.38	0	1.03	0.34
K2SF	67.59	0.05	18.88	2.88	1.28	0.73
K4SF	69.07	0.05	18.49	2.91	1.33	0.73
K6SF	70.55	0.08	18.12	2.94	1.38	0.73
K6SF3ESA	60.64	1.95	17.54	2.85	1.36	0.73
K6SF6ESA	62.62	3.82	16.97	2.77	1.35	0.69
K6SF9ESA	64.6	5.69	16.39	2.68	1.33	0.66
K6SF3L	62.02	7.54	17.55	2.87	1.38	0.69
K6SF6L	63	9.41	16.98	2.79	1.36	0.64
K6SF9L	64.21	11.28	16.41	2.73	1.33	0.61
K6SF6ESA3L	64.51	13.15	14.39	2.72	1.32	0.58
K6SF6ESA6L	67.32	15.02	10.59	2.69	1.3	0.54
K6SF6ESA9L	69.31	16.89	9.23	2.64	1.27	0.49

The constant pozzolanic response generates gel-like (CSH- calcium silicate hydrates) and threadlike (CAH- calcium aluminates hydrates) cementing synthesis, which strengthens the coalition between the treated kaolin clay molecules and substantiates the soft kaolin clay strength. According to Table 2, 62.5% of ESA and 72.6% of L are mainly composed of CaO, while 74.02% of SF is made up of SiO_2. In this investigation, CSH and CAH can be generated with $Ca(OH)_2$ from ESA and L; and SiO_2, Al_2O_3 from SF and soft kaolin clay in a presence of the moisture environment. The composition analysis of SF, ESA and L with respect to the SiO_2 content and the CaO content is identical to the chemical composition of SF (SiO_2 = greater than 85.0%; CaO = < 1.0%), ESA (SiO_2 = < 1.0%; CaO = 33.1% - 99.8%) and L (SiO_2 = 0.4% - 15.4%; CaO = greater than 43.8%) examined by Sathiparan (2021).

Subsequently, SF accommodates a substantial amount of silica and it is an exemplary pozzolan that can be used as one of the soil stabilizing agent. Furthermore, ESA and L retaliate with a pozzolanic element to structure the Ca_2SiO_4 (calcium silicate) paste. The CSH acts instantly to inlay and cohere kaolin clay fragments in the kaolin clay and to occlude the soil lacuna. In addition, ESA and L slowly reshape from the gel state to lucid state, resulting in interlocking between the molecules of the problematic soil. Nevertheless, this gel moderately crystallizes into CSH namely as tobermorite and hillebrandite, which can increase the strength and diminish the swelling of the soft kaolin clay.

Furthermore, the augmentation and contraction of soft kaolin clay is predominantly due to the moisture integration of an extensive mineral in soft kaolin clay that will alter the thickness of the soil moisture film. The reduction in thickness leads to a greater cohesive force between the molecules, an increase in soil shear strength, and a smaller shrinkage characterisation. Therefore, due to the coagulation reaction and ion interchange, the combinations of SF-ESA-L are sufficient to improve soil utilisation to establish the fundamental requirement for pozzolanic materials and cementitious materials to produce cementitious composites.

3.5 Mineralogical Characteristics of Raw, Treated and Untreated Soft Kaolin Clay

XRD analysis assisted in the conception of the mineral alterations, which occurred in soft kaolin clay on the inclusion of SF, ESA and L in terms of crystalline stages, physical characterisation of single elements, and the ideal combination. The dominant minerals for soft kaolin clay comprised of quartz, kaolinite, and illite, cristobalite for the SF, calcite and portlandite for the ESA and L, and kaolinite, quartz, calcite, cristobalite, and muscovite for the optimum amalgamation. SiO_2 were inherited dominantly from SF. The XRD patterns of soft kaolin clay, SF, ESA, and L illustrated in Figs. 10 (a) to 10 (d), indicated the formation of new peaks based on the mineralogical compositions of the utilised materials. Identical investigations have been examined by Hasan et al., (2021c) on the behaviour of SF and ESA stabilisers in soft kaolin clay.

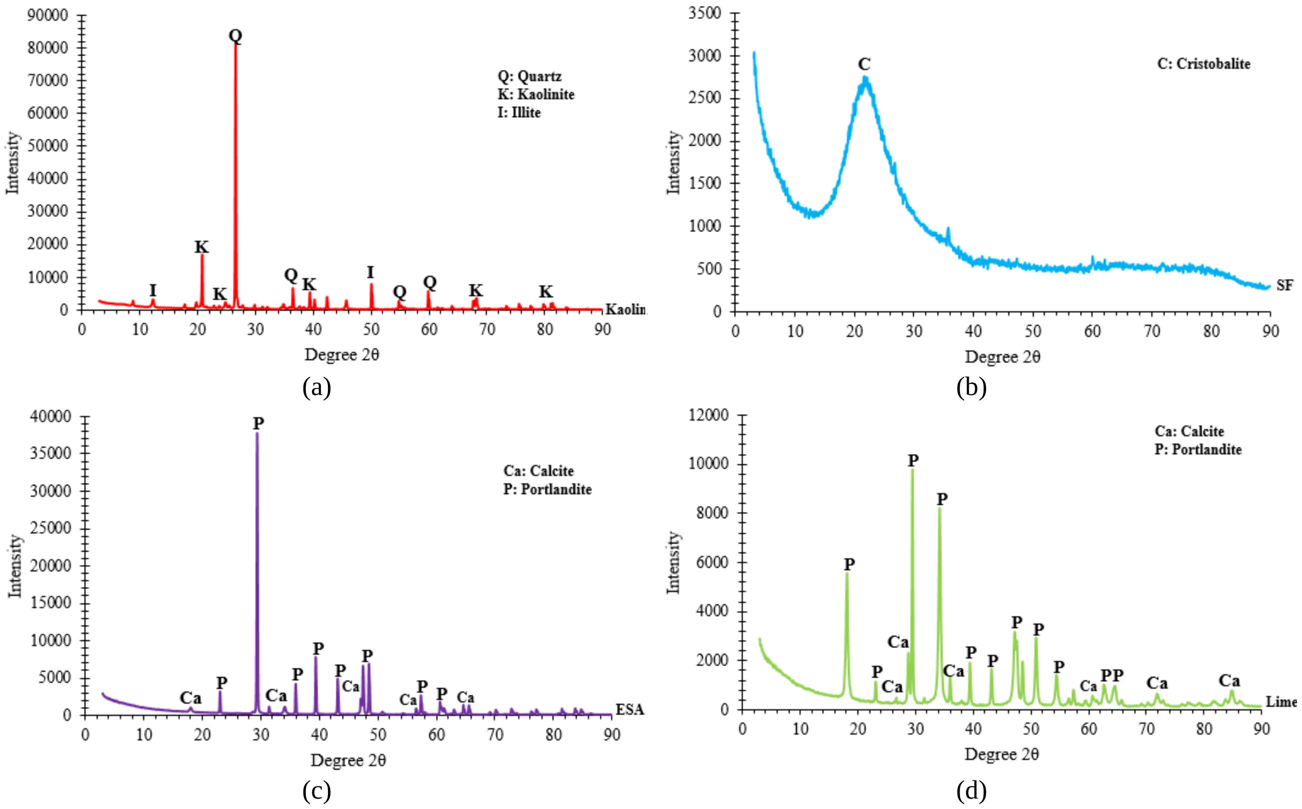

Fig. 10 - X-ray Diffraction Pattern of: a) Soft Kaolin Clay; b) Silica Fume; c) Eggshell Ash; d) lime

Fig. 11 demonstrates the XRD analysis of treated soft kaolin clay with different ratios of SF, SF-ESA, SF-L and combinations of SF-ESA-L. The primary mineralogical components of soft kaolin clay are kaolinite and quartz, while illite is the minor phases. Jafer et al. (2018) stated that most recurrent crystalline clay minerals comprise kaolinite, illite, smectite, and montmorillonite. Differentiation between the maximum points of soft kaolin clay as the primary material and the combination of soft kaolin clay with SF, SF-ESA, SF-L, and SF-ESA-L shows that the peak points of the quartz and kaolinite (see Fig. 11) are slightly reduced than the untreated soft kaolin clay due to the establishment of the cementation amalgamation. Furthermore, based on the XRD pattern of the optimal mixture, CSH as a primary hydration by-product was not discovered due to the amorphous surrounding of this by-product (Zaini et al., 2020b). The presence of CaO in the calcite and portlandite mineral of ESA and L enhanced the strength potential of the soft kaolin clay. The hydration of the CaO produces $Ca(OH)_2$ which interconnect with the subsist of CO_2 in the surrounding. This reaction produces $CaCO_3$ through a carbonation mechanism that increases the soil molecule bonding rate of soil molecules and has a substantial function of increasing the strength of the soft kaolin clay. In addition, amalgamating calcite and portlandite with the wet clay particle in the presence of cristobalite divides it into calcium, silicate, aluminate, and hydroxide ions. Negative charges of soft kaolin clay were absorbed by positive charges of the Ca causing soft kaolin clay molecules to congregate and eventually improving the coalition among soft kaolin clay molecules and increasing the strength (Kalhor et al., 2022). Similar results have been reported by Zaini et. al., (2022a).

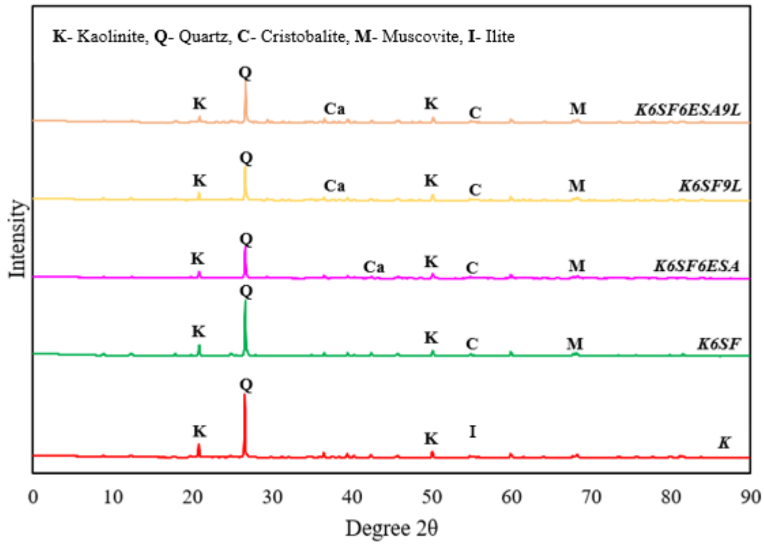

Fig. 11 - X-ray diffraction pattern of treated soft kaolin clay with different ratios and combination of SF, ESA and L

3.6 Morphological Characteristics of Untreated and Treated Soft Kaolin Clay

Table 3 illustrates the particle size distribution (PSD) of the untreated soft kaolin sample and the treated soft kaolin clay with a different ratio of SF, ESA and L for the optimum stabiliser. Untreated kaolin shows that there is 38.4% of particles that are equal or smaller than 0.075 mm while 61.6% are between 0.075 mm and 4.75 mm particle size. According to Table 3, when soft kaolin clay was treated with 6% SF, 6% SF and 6% of ESA, 6% of SF and 9% of L and 6% of SF, 6% of ESA and 9% L, the quantity of soil that was retained at 0.075 mm to 4.75 mm increases from 61.6% to 76.6%, which shows that the soil particles became coarser with the reduction of the particle size retained at 0.075 mm to 23.4% from 38.4%. The size of the particles of the SF can be classified as MH, sandy soil with a high plasticity. Moreover, ESA exists under a coarser condition ranging from 0.063 to 0.3 mm, with 25% of the particles passing the 0.075 mm sieve, while 75% of it retained above the 0.075 mm sieve. ESA is classified as SC, sandy-clay particles and is classified as A-2-4 based on the AASHTO classification due to its consistency limit properties.

Table 3 - PSD of untreated kaolin sample, SF, ESA and treated kaolin sample admixed with 6% SF and 6%

Particle Size (mm)		> 4.75	0.075 – 4.75	≤ 0.075
Cumulative Passing (%)	**Kaolin**	0	61.6	38.4
	K6SF	0	68.2	31.8
	K6SF6ESA	0	67.4	32.6
	K6SF9L	0	76.6	23.4
	K6SF6ESA9L	0	76.6	23.4

The incorporation of SF, ESA, and L to stabilise kaolin clay induced the restructuring of the kaolin clay molecule, establishing a coarser kaolin fusion where the sieve graph of the treated kaolin clay transposes vaguely to the coarser side (see Fig. 12). Improved soft kaolin clay is categorised as sand-silt soil (SM) and is classified as sandy-silt (A-2-4) according to AASHTO. It consists of 0% gravel, 68.2% fine sand and 31.8% clay and silt when treated with 6% SF, 0% gravel, 67.4% fine sand and 32.8% clay and silt when treated with 6% of SF and ESA, 0% gravel, 76.6% fine sand, and 23.4% of clay and silt when treated with 6% of SF, 9% of L and the combination of ESA-L. According to the UCT result obtained from Section 3.3.1, the highest pozzolan and CaO content that results in the highest USS is achieved by using 6% of SF, 6% of ESA, and 9% of L. Similar results have been investigated by Hasan et al. (2021c) and Zaini et. al., (2022a) on the morphology analysis of SF and ESA.

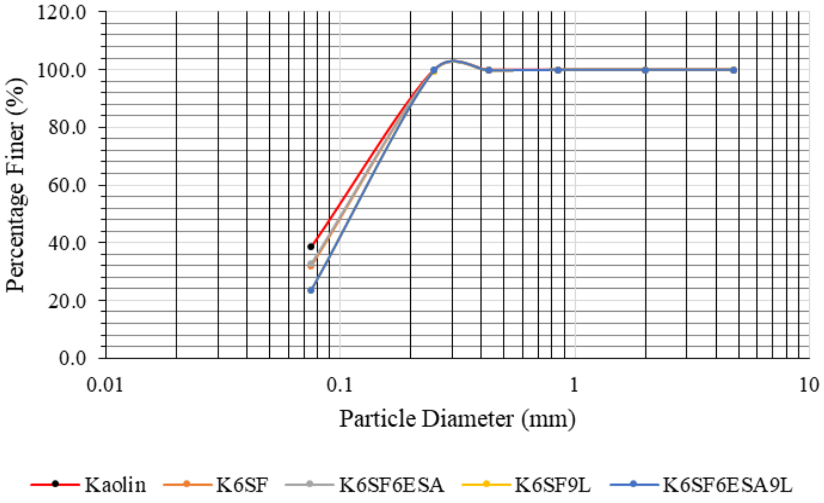

Fig. 12 - Effect of using SF, ESA and L to the PSD curve of the soft kaolin clay

3.7 Microstructural Characteristics of Treated and Untreated Soft Kaolin Clay

Microstructural analysis was performed to examine the nanostructures figurine of soft kaolin clay, SF, ESA, L and treated soft kaolin clay at the optimal utilization of SF, ESA and L. FESEM images of untreated soft kaolin clay, SF, ESA and L are demonstrated in Fig. 13(a) to Fig. 13(d) while Fig. 15(a) to Fig. 15(d) illustrate the microscopic condition of soft kaolin clay when treated with 6% of SF, 6% of SF and 6% of ESA, 6% of SF and 9% of L and 6% of SF and ESA and 9% of L. Soft kaolin clay has a scabrous-shaped microstructure, while the SF molecule has a tiny globular shape with a molecule size of thousand micrometres. The ESA and L molecules appeared to be identical because they had a rocky, scattered morphology and a fluctuating molecule size apportionment. Similar microscopic analysis has been examined by Hasan et. al., (2021c) and Sharma et al. (2018).

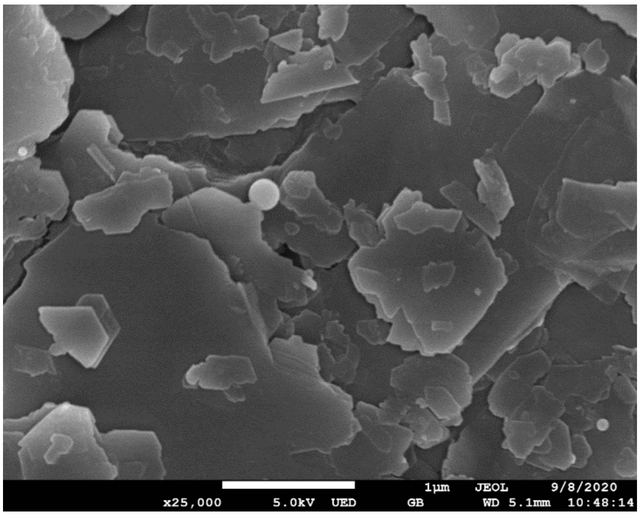

(a)

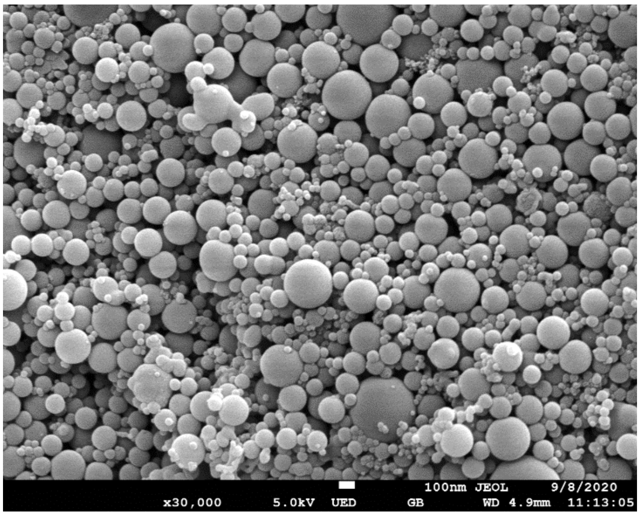

(b)

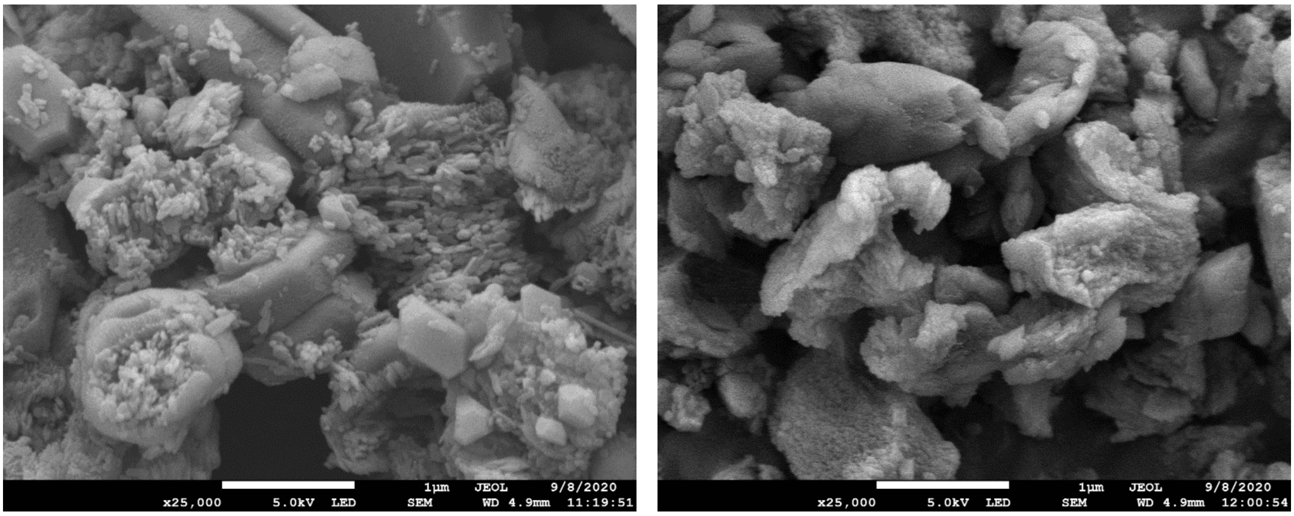

(c) (d)

Fig. 13 - FESEM image analysis of: a) soft kaolin clay under 25 000 magnification; b) SF under 30000 magnification; c) ESA under 25 000 magnification and; d) L under 25000 magnification

The inclusion of ESA and L is identical sequel to morphological alterations. Based on Figs. 15(a) to 15(d), it can be examined that the scabrous and even molecules of soft kaolin clay shatter into uneven lumps upon the inclusion of SF, ESA, and L. This strengthens the linkage between the molecules, and enhances the strength and diminish the plasticity indices. Identical investigations have been studied by Sharma et al. (2018) on the effect of lime on clays and Zaini et. al., (2022a) on the effect of ESA on the soft kaolin clays. The establishment of unpigmented cementitious amalgamation (CAH and CSH) on the surfaces of clay molecules acts as a criterion for pozzolanic reactivity (see Figs. 15(a) to 15(d)). Similar establishments have been reported for numerous types of soil (Dash & Hussain, 2015). Ca^{2+}, proffer by ESA and L, retaliate with the alumina and silica that exist in SF and kaolin throughout the pozzolanic reaction (Dash & Hussain, 2015). Additionally, the flocculation and aggregation mechanism has taken place in the soft kaolin clay molecules when ESA and L are used as the microstructure of the soft kaolin clay is altered (see Fig. 15(d)).

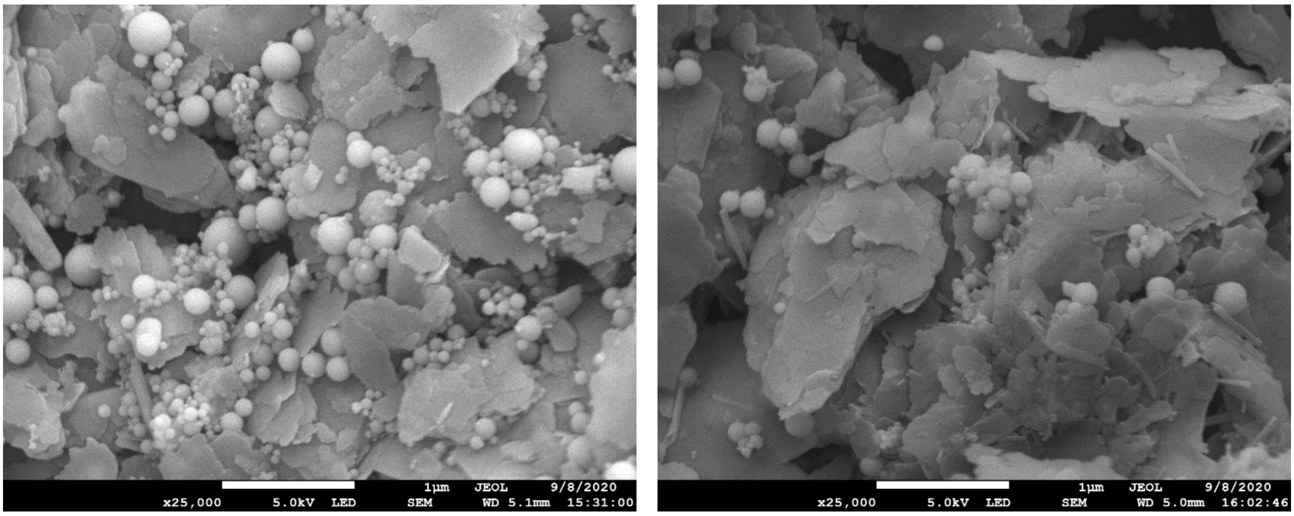

(a) (b)

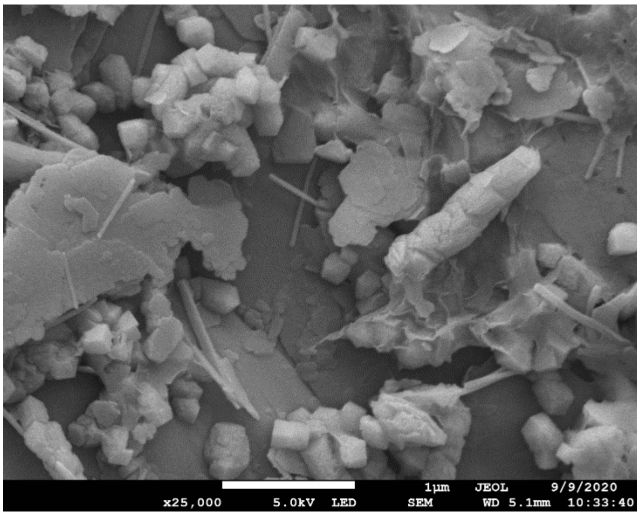

(c)

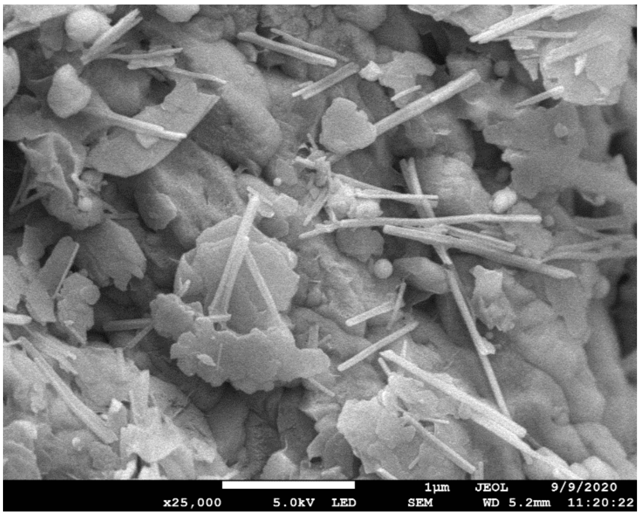

(d)

Fig. 16 - Morphological microstructure of soft kaolin clay; a) treated with 6% of SF under 25000 magnification; b) Treated with 6% SF and 6% of ESA under 25000 magnification; c) Treated with 6% of SF and 9% L under 25000 magnification and; d) Treated with 6% of SF, 6% of ESA and 9% of L under 25000 magnification

4. Conclusions

This investigation examined the influence of SF, ESA, and lime on the alterations of soft kaolin clay characteristics. Kaolin clay can be classified as ML, which indicates as low plasticity silt with a liquid limit (LL) of 40.9%, plastic limit (PL) of 33.3%, and plasticity index (PI) of 7.6%. The specific gravity of kaolin clay recorded at 2.64 and shrinkage limit (SL) of 23.93%. Furthermore, the MDD of kaolin was 1.55 kg/m^3 with an OMC of 21.00%. Soft kaolin clay with SF-ESA-L falls into the category A-4 - 4 group, which predominantly contains fine sand and was classified as sandy soil (SM) with a specific gravity of 2.38 and SL of 26.31%. Furthermore, the LL, PL and PI of the treated soft kaolin clay with optimal use of SF-ESA-L is 36.6%, 32.7% and 3.9% respectively. The MDD of the soft kaolin clay with SF-ESA-L was 0.64 kg/m^3 with an OMC of 21.00%. Moreover, The shear strength of the soft clay was substantially affected by optimal utilisation of SF-ESA-L. The use of SF-ESA-L in a 6:6:9 ratio significantly improved the shear strength of soft kaolin clay from 13.154 kN/m^2 to 69.344 kN/m^2 with a strength improvement of 81.03%. The increase in the strength of the treated soft kaolin clay soil was due to the adequate portion of amorphous silica and alumina in the SF that triggered the pozzolanic reactivity of the soil. However, the interchange reaction of the flocculation of kaolin clay molecules, the pozzolanic reactivity, and agglomeration are the main physiochemical reactions that regulate the engineering characteristics of kaolin-treated mixtures. Dissociation and interchange of cations assist in instantaneous alterations in the workability of the soil, which strengthen the link between the soil molecules and improve the strength properties of the soft kaolin clay. Therefore, the study concludes that the utilisation of SF, ESA and lime rigidly affected various properties of kaolin clay as an effective soil binder. Therefore, it is advocated that the utilisation of 6% SF, 6% ESA, and 9% of lime as a problematic soil strength enhancement to alter the kaolin clay characteristics for construction application can be reached up to 88.74% at 30 days of curing.

Acknowledgement

The authors would like to acknowledge the Universiti Malaysia Pahang (UMP) and Hokoko Engineering Co. Ltd for financing this research through the International Grant, Project Number UIC201503, UMP Matching Grant, Project Number RDU202701, RDU223309 and Postgraduate Research Grant Scheme (PGRS), Project Number PGRS2003185. The cooperation given by all parties involved in this research is greatly acknowledged.

References

Ali, B., Ouni, M.H.E., & Kurda, R (2022). Life cycle assessment (LCA) of precast concrete blocks utilizing ground granulated blast furnace slag. *Environmental Science and Pollution Research, 29,* pp. 83580-83595.

Alnunu, M.Z., & Nalbantoglu, Z (2022). Performance of Using Waste Marble Dust for the Improvement of Loose Sand in Deep Soil Mixing. *Arabian Journal of Science and Engineering, 47,* pp. 4681–4694.

Araujo, M.T., Ferrazo, S.T., Chaves, H.M., Rocha, C.G., & Consoli, N.C (2023). Mechanical behavior, mineralogy, and microstructure of alkali-activated wastes-based binder for a clayey soil stabilization. *Construction Building Materials, 362,* pp.129757.

American Society for Testing and Materials (2016). *Standard Test Method for Unconfined Compressive Strength of Cohesive Soil*. ASTM E1621-16

American Society for Testing and Materials (2013). *Standard guide for elemental analysis by wavelength dispersive X-Ray fluorescence spectrometry*. ASTM E1621-13

American Society for Testing and Materials (2019). *Standard Test Method for Determination of Relative X-ray Diffraction Intensities of Faujasite-Type Zeolite-Containing Materials*. ASTM D3906-19

American Society for Testing and Materials (2014). *Standard Test Method for Particle-Size Analysis of Soils*. ASTM D422-63

Bagriacik, B (2021). Utilization of alkali-activated construction demolition waste for sandy soil improvement with large-scale laboratory experiments. *Construction Building Materials, 302*, pp.124173.

Blayi, R.A., Sherwani, A.F.H., Ibrahim, H.H., H. Faraj Rabar & Daraei A (2020). Strength improvement of expansive soil by utilizing waste glass powder. *Case Studies in Construction Materials, 13,* pp. e00427.

Bozyigit, I., Javadi, A., & Altun, S (2021). Strength properties of xanthan gum and guar gum treated kaolin at different water contents. *Journal of Rock Mechanics and Geotechnical Engineering, 13*(5), pp. 1160-1172.

Brescia-Norambuena, L., González, M., Avudaiappan, S., Saavedra Flores E. I., & Grasley Z (2021). Improving concrete underground mining pavements performance through the synergic effect of silica fume, nanosilica, and polypropylene fibers. *Construction and Building Materials, 285,* pp.122895.

British Standards Institution (2010). *Methods of test for soils for civil engineering purposes. Part 2: Classification tests*. BS 1377-2:1990

Chemeda, Y.C., Deneele, D., & Ouvrard, G (2018). Short-term lime solution-kaolinite interfacial chemistry and its effect on long-term pozzolanic activity. *Applied Clay Science, 161,* pp.419-426.

Dash, S.K., & Hussain, M. Influence of Lime on Shrinkage Behavior of Soils (2015). *Journal of Materials in Civil Engineering, 27*(12), pp.04015041.

Goh, J.R., Ishak, M.F., Zaini, M.S.I., & Zolkepli, M.F (2020). Stability analysis and improvement evaluation on residual soil slope: Building cracked and slope failure. *IOP Conference Series: Materials Science and Engineering,* 2020. pp.072017.

Hamada, H., Tayeh, B., Yahaya, F., Muthusamy K., & Al-Attar A. (2020). Effects of nano-palm oil fuel ash and nano-eggshell powder on concrete. *Construction and Building Materials, 261,* pp.119790.

Hasan, M., Zaini, M.S.I., Hashim, N.A.A., Wahab, A., Masri, K.A., Jaya, R.P., Hyodo, M., Winter, M.J., Sholichin, M., & Haribowo, R. (2021a). Stabilization of Kaolin Clay Soil Reinforced with Single Encapsulated 20mm Diameter Bottom Ash Column. *IOP Conference Series: Earth and Environmental Science*, 2021, pp.012099

Hasan, M., Zaini, M.S.I., Hong, N.A.W., Wahab, A., Masri, K.A., Jaya, R.P., Hyodo, M., Winter, M.J., Sholichin, M., & Haribowo, R. (2021b). Sustainable ground improvement method using encapsulated polypropylene (PP) column reinforcement. *IOP Conference Series: Earth and Environmental Science*, 2021, pp.012016.

Hasan, M., Zaini, M.S.I., Yie, L.S., Masri, K.A., Jaya, R.P., Hyodo, M., & Winter, M.J. (2021c). Effect of optimum utilization of silica fume and eggshell ash to the engineering properties of expansive soil. *Journal of Materials Research and Technology, 14,* pp.1401-1418.

Hilal, N., & Hadzima-Nyarko, M. (2021). Improvement of eco-efficient self-compacting concrete manufacture by recycling high quantity of waste materials. *Environmental Science and Pollution Research, 28,* pp.53282–53297.

Ishak, M.F., & Zaini, M.S.I (2018). Physical Analysis Work for Slope Stability at Shah Alam, Selangor. *Journal of Physics: Conference Series,* 2018, pp.012064.

Ishak, M.F., Zolkepli, M.F., Yunus, M.Y.M., Ali, N., Kassim, A., & Zaini, M.S.I (2021). Verification of tree induced suction with numerical model. *Physics and Chemistry of the Earth, 121,* pp.102980.

Jafer, H., Atherton, W., Sadique, M., Ruddock, F., &Loffill, E. (2018). Stabilisation of soft soil using binary blending of high calcium fly ash and palm oil fuel ash. *Applied Clay Science, 152,* pp.323-332.

Kalhor, A., Ghazavi, M. & Roustaei, M. (2022). Impacts of Nano-silica on Physical Properties and Shear Strength of Clayey Soil. *Arabian Journal of Science and Engineering, 47*, pp.5271–5279.

Mahmutluoğlu, B., & Bağrıaçık, B (2022). Utilization of Alkali-Activated Glass Manufacturing Waste in the Improvement of Cohesive Soils. *Arabian Journal of Science and Engineering, 47*, pp.12765–12778.

Mohammed, M.A., Mohd Yunus, N.Z., Hezmi, M.A., Abang Hasbollah, D.Z., & A. Rashid, A.S. (2021). Ground improvement and its role in carbon dioxide reduction: a review. *Environmental Science and Pollution Research, 28,* pp.8968–8988.

Ofuyatan, O.M., Adeniyi, A.G., Ijie, D., Ighalo, J.O., & Oluwafemi, J. (2020). Development of high-performance self compacting concrete using eggshell powder and blast furnace slag as partial cement replacement. *Construction and Building Materials, 256,* pp.119403.

Poorveekan, K., Ath, K.M.S., Anburuvel, A., & Sathiparan, N. (2021). Investigation of the engineering properties of cementless stabilized earth blocks with alkali-activated eggshell and rice husk ash as a binder. *Construction and Building Materials, 277,* pp.122371.

Sathiparan, N. (2021). Utilization prospects of eggshell powder in sustainable construction material – A review. *Construction and Building Materials, 293,* pp.123465.

Sharma, L.K., Sirdesai, N.N., Sharma, K.M., & Singh, T.N. (2018). Experimental study to examine the independent roles of lime and cement on the stabilization of a mountain soil: A comparative study. *Applied Clay Science, 152,* pp.183-195.

Tiong, H.Y., Lim, S.K., Lee, Y.L., Ong, C.F., & Yew, M.K. (2020). Environmental impact and quality assessment of using eggshell powder incorporated in lightweight foamed concrete. *Construction and Building Materials, 244,* pp.118341.

Türköz, M., Umu, S.U., & Öztürk, O. (2021). Effect of silica fume as a waste material for sustainable environment on the stabilization and dynamic behavior of dispersive soil. *Sustainability*, *13*(8), pp.4321.

Yue, L.J., Ishak, M.F., Zaini, M.S.I., & Zolkepli, M.F. (2019). Rainfall induced residual soil slope instability: Building cracked and slope failure. *IOP Conference Series: Materials Science and Engineering,* 2019, pp.012004.

Zaini, M.S.I., Ishak, M.F., & Zolkepli, M.F. (2019).Forensic assessment on landfills leachate through electrical resistivity imaging at Simpang Renggam in Johor, Malaysia. *IOP Conference Series: Materials Science and Engineering,* 2019, pp.012005.

Zaini, M.S.I., Ishak, M.F., Zolkepli, M.F. (2020a). Monitoring soil slope of tropical residual soil by using tree water uptake method. *IOP Conference Series: Materials Science and Engineering,* 2020, pp.072018

Zaini, M.S.I., Ishak, M.F., Zolkepli, M.F. et al (2020b). Granite Exploration by using Electrical Resistivity Imaging (ERI): A Case Study in Johor. *International Journal of Integrated Engineering*, *12*(8), pp.328-347.

Zaini, M.S.I., Hasan, M., Yie, L.S., Masri, K.A., Jaya, R.P., Hyodo, M., & Winter, M.J. (2022a). THE EFFECT OF UTILIZING SILICA FUME AND EGGSHELL ASH ON THE GEOTECHNICAL PROPERTIES OF SOFT KAOLIN CLAY. *Jurnal Teknologi*, *84*(1), pp.159-170.

Zaini, M.S.I., Hasan, M., & Zolkepli, M.F. (2022b). Urban landfills investigation for leachate assessment using electrical resistivity imaging in Johor, Malaysia. *Environmental Challenges, 6,* pp.100415.

Zaini M. S. I., Hasan M., & Jusoh, W. N. B. W. (2023). Utilization of bottom ash waste as a granular column to enhance the lateral load capacity of soft kaolin clay soil. *Environmental Science and Pollution Research*.

Zaini M.S.I., & Hasan M. (2023). Effect of Optimum Utilization of Silica Fume and Lime on the Stabilization of Problematic Soils. *International Journal of Integrated Engineering*.

Zolkepli, M.F., Ishak, M.F., Zaini, M.S.I. (2018). Analysis of slope stability on tropical residual soil. *International Journal of Civil Engineering and Technology, 9*(2), pp.402-416.

Zolkepli, M.F., Ishak, M.F., Zaini, M.S.I. (2019). Slope stability analysis using modified Fellenius's and Bishop's method. *IOP Conference Series: Materials Science and Engineering*, 2019, pp.012004

Zolkepli, M.F., Ishak, M.F., Yunus, M.Y.M., Zaini, M.S.I., Wahap, M.S., Yasin, A.M., Sidik, M.H., & Hezmi, M.A., (2021). Application of unmanned aerial vehicle (UAV) for slope mapping at Pahang Matriculation College, Malaysia. *Physics and Chemistry of the Earth, 123,* pp.103003.